COLUMBIA POWER TECHNOLOGIES

Direct Drive Wave Energy Buoy

Title	Metocean Report
Document No.	S1-DB-01
Version	4.1
Authored	P Lenee-Bluhm
Reviewed	Z. Zhang
Approved	K. Rhinefrank

Version	Date	Summary
1.0	December 17, 2012	Release to Garrad Hassan for comment
2.0	July 9, 2013	Release for Design Basis submission to Germanischer Lloyd
3.0	October 4, 2013	Re-release following comments by GLRC
3.1	December 10, 2013	Add normal current speed and misc edits
3.2	February 13, 2014	Re-release following comments by GLRC
4.0	October 27, 2014	Updated source of data for operational seas (2.1), complete revision of Operational Seas (2.2), some revisions to Extreme Seas (2.3), and added marine growth (8). WEC assumed to operate at 80m depth (not 70m).
4.1	5 June, 2015	Added directional scatter tables as appendix

TABLE OF CONTENTS

TABLE OF FIGURES

TABLE OF TABLES

1 INTRODUCTION

Columbia Power Technologies, Inc. (CPwr) is developing a Wave Energy Converter (WEC) for utility-scale power applications. Dubbed the StingRAY v3.2, this latest version of the RAY series WEC represents a number of design optimizations aimed to reduce system loading and increase power production. CPwr is currently working towards Prototype certification of this WEC. The purpose of this document is to describe the bathymetry and bottom conditions at the U.S. Navy Wave Energy Test Site (WETS) at Kaneohe Bay, Hawaii, along with the metocean conditions that the WEC may be expected to be exposed to while deployed there.

Section 3.B.200 of DNV-OSS-312 *Certification of Tidal and Wave Energy Converters* (2011) [1] was consulted to provide an overview of environmental data required as a basis for design; based on recommendations therein, this document is organized into the following sections:

- Introduction
- Waves
- Wind
- Current
- Tide
- Bathymetry and Bottom Conditions
- Marine Growth
- Temperature

In general, Section 1 of GL Rules and Guidelines IV-6-4 *Offshore Structures: Structural Design* (2007) [2] and DNV-RP-C205 *Environmental Conditions and Environmental Loads* (2010) [3] were consulted for technical definitions related to environmental conditions. These and additional references shall be cited where appropriate.

2 WAVES

2.1 Site Location and Sources of Data

WETS is located on the northeast side of Oahu at Kaneohe Bay. There are two deep water test berths planned. Berths A and B are planned to be centered at locations with depths of 60 and 80 m, respectively, as shown in Figures 1 and 2. The two sites are approximately 920 m apart. CPwr has been awarded the use of berth B, thus the design is based on berth B. The locations of the berths are specified in Table 1. The center of test berth B, which coincides with the position of the deployed WEC, is at a depth of 80 m.

The waves incident on the Hawaiian Islands are dominated by swell from the northwest and south, and wind waves from the northeast [4]. As Figures 1 and 2 make clear, the test site is entirely shielded from the south swell, and shielded from some components of northwest swell and east wind waves.

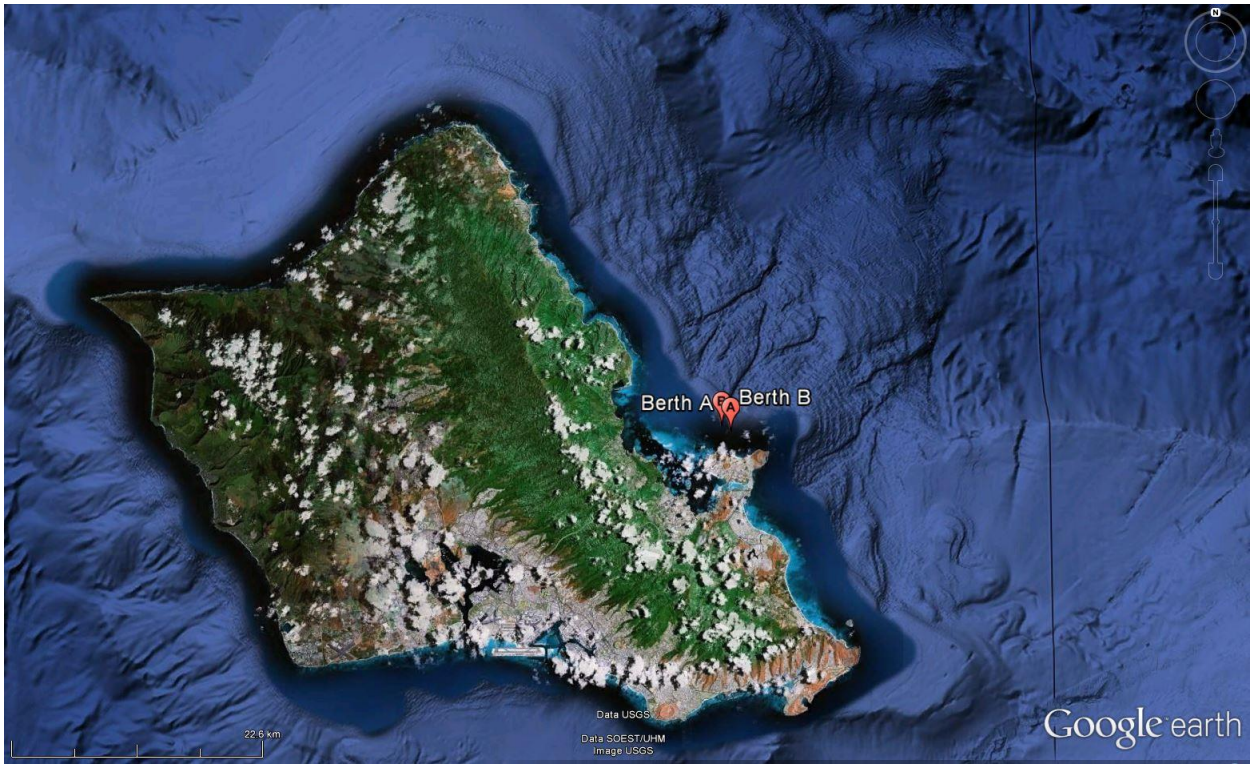

Figure 1 – General location of WETS deep water test berths.

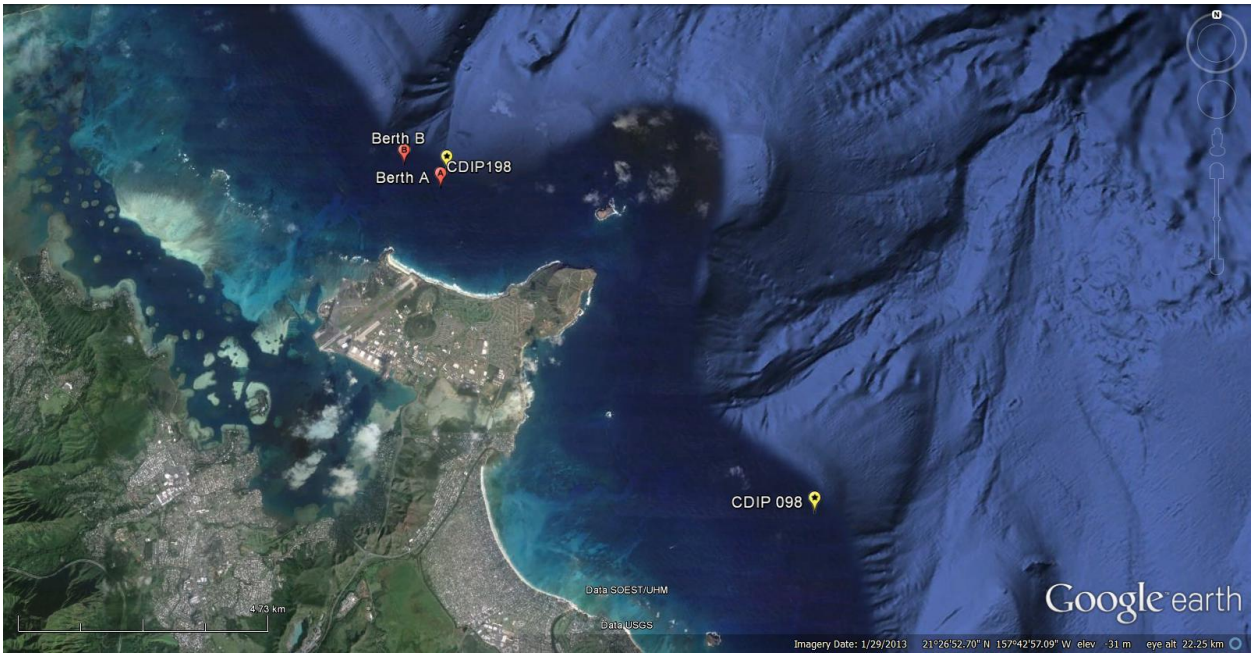

Figure 2 – Location of deep water test berths and sources of measured and modeled wave data.

Nearby Waverider buoys, owned and maintained by Pacific Islands Ocean Observing System (PacIOOS) with data archived online by the Scripps Institution of Oceanography, are indicated by station ID numbers CDIP 098 and CDIP 198 in Figure 2. This data is archived online by the Scripps Institution of

Oceanography and is available as half-hourly spectral wave records. The locations of the wave measurement buoys, and the availability of their records over the time spans utilized by CPwr, are specified in Table 1. A CPwr internal report [5] shows that the wave conditions observed at CDIP 098 and CDIP 198 from Oct 2012 to May 2013 are fairly similar, though the differences are not insignificant. Mean significant wave height, H_{m0}, at CDIP 098 is 16% greater than at CDIP 198. The difference in wave height is greatest when the dominant wave direction observed at 098 is east to southeast, as waves from this heading will encounter Mokapu Point en route to 198. A comparison of the most energetic storm peaks (three events where H_{m0} observed at either station exceeded 4.5 m, all from the northeast) revealed that for this sub-dataset H_{m0} tended to be greater at CDIP 098; H_{m0} at CDIP 098 was observed to be between 8% less than to 19% more than H_{m0} at CDIP 198, with a mean H_{m0} roughly 7% greater.

Frequency-directional spectral wave data, obtained by a phase-averaged wave propagation model run by Hawaii National Marine Renewable Energy Center (HINMREC), was made available to CPwr. SWAN v40.85 was forced with 34 years of spectral wave data from global model WAVEWATCH III (WW3) v4.08. The WW3 model was forced using Climate Forecast System Reanalysis winds globally and high resolution Weather and Forecasting (WRF) winds for the Hawaii region. The resolution of the Oahu SWAN model was 550 m; interpolation of the four nearest grid points yielded spectral output coincident with CDIP 198 (as specified in Table 1). Model validation against 11 months of CDIP 198 measurements indicate general agreement, though the model underestimates large swells above 3.5 m significant wave height [6]. More extensive reporting on the modeling and validation is currently under internal HINMREC review (as of Oct 2014), and will be referenced in a revision of this report when available.

Table 1 – Locations of WETS berths and sources of wave data.

Identity	Latitude [N]	Longitude [W]	Depth [m]	Extent of record	Availability
Berth A	21°28'27.24"	157°45'13.54"	60	N/A	N/A
Berth B	21°28'43.24"	157°45'40.59"	80	N/A	N/A
CDIP 098	21°24'51.00"	157°40'43.80"	90	Aug 2000 – May 2013	91%
CDIP 198	21°28'39.00"	157°45'9.60"	81	Oct 2012 – May 2013	99%
Model node	Same as CDIP 198			Jul 1979 – Jun 2013	100%

The primary dataset utilized for characterization of the waves at the test site is the SWAN model output at the model node specified in Table 1 (coincident with CDIP 198). This 34 year dataset is used to characterize the expected operational seas incident at the test site. The slight differences in location (920 m) and water depth (1 m) between the model node and berth B are assumed insignificant, and no wave shoaling correction was applied H_{m0} associated with extreme seas (e.g. 50 year return storm height) will be derived from the 13 year dataset measured at CDIP 098. The underestimation of the largest wave heights by the model, along with the similarity of wave records between CDIP 098 and 198, render the measured dataset from the CDIP 098 the best available dataset for estimation of extreme seas. It is assumed that the extreme seas estimates thus obtained will be conservative for the test location.

2.2 Operational Seas

Spectral wave data were provided by Hawaii National Marine Renewable Energy Center (HINMRC). For each of the hourly spectra, the two-dimensional frequency-directional wave elevation variance density, S_{fd}, was provided. The spectra were discretized over 26 exponentially increasing frequency bins, f, whose centers range from 0.0418 to 1.0 Hz and 24 equal directional bins, θ, that cover a full 360°. Wave direction is presented as positive clockwise from true north. A total of 34 years of hourly data were utilized, beginning with Jul 1, 1979 and ending with Jun 30, 2013, for a total of 298,055 records.

The parameterization of the sea states presented here follows the recommendations of IEC 62600-101 *Wave Energy Resource Assessment and Characterization* (2014) [7]. Note that as of Oct 2014 this IEC document is a draft, but it is expected to be published as a Technical Specification in a matter of months.

As directionally unresolved characteristic parameters are more readily calculated using the one-dimensional frequency variance densities, S_f, these are first calculated as

$$S_f = \int_\theta S_{fd}\, d\theta \tag{1}$$

This and all other integrations are performed numerically, with bin widths and centers defined for each frequency and direction bin.

Wave height is characterized by the significant wave height, H_{m0}, and is calculated as

$$H_{m0} = 4\sqrt{m_0} \tag{2}$$

where m_0 is the zeroth moment of the frequency spectrum, and any n^{th} order moment, m_n, is calculated as

$$m_n = \int_f f^n\, S_f\, df \tag{3}$$

Wave period is primarily characterized by the energy period, T_e, and is calculated as

$$T_e = m_{-1}/m_0 \tag{4}$$

Another wave period parameter is the mean zero-crossing period, T_z, which is calculated as

$$T_z = \sqrt{m_0/m_2} \tag{5}$$

Sea state steepness is characterized using the significant steepness, S_s, which is calculated as

$$S_s = \frac{2\pi H_{m0}}{gT_z^2} \tag{6}$$

where g is the acceleration due to gravity (assumed to be 9.81 m/s^2).

The incident omnidirectional wave power, J, is defined as the wave energy transport rate per unit width from the sea floor to the surface, and is calculated as

$$J = \rho g \int_f S_f\, c_g\, df \tag{7}$$

where ρ is the density of sea water (assumed to be 1025 kg/m^3), and c_g is the group velocity for which the depth dependent calculation can be seen in Table 3-1 of [3].

The spectral width, ϵ_0, is a non-dimensional parameter that characterizes the spreading of energy over the frequency spectrum, and is calculated as

$$\epsilon_0 = \sqrt{\frac{m_0 m_{-2}}{m_{-1}^2} - 1} \tag{8}$$

Resolving the incident wave power associated with the frequency-directional spectrum to a given direction, α, yields the directionally resolved wave power, J_α, which is defined as the wave energy transport rate through an envisioned vertical plane of unit width, extending from the sea floor to the surface, whose normal

vector is parallel with α. The directionally resolved wave power is calculated as the sum of the of the contributions of each sea state component that resolves positively in direction α, as

$$J_\alpha = \rho g \iint_{f,\theta} S_{fd}\, c_g\, df d\theta \cos(\theta - \alpha)\, \delta \qquad \begin{cases} \delta = 1, \cos(\theta - \alpha) \geq 0 \\ \delta = 0, \cos(\theta - \alpha) < 0 \end{cases} \tag{9}$$

J_α was calculated at 1° increments; the maximum value is denoted as $J_{\theta Jmax}$ and characterizes the maximum directionally resolved wave power. The direction of the incident sea state is characterized using the direction associated with $J_{\theta Jmax}$; this parameter is called the direction of maximum directionally resolved wave power and is denoted as θ_{Jmax}.

The degree to which the incident wave power is spread directionally is characterized by the directionality coefficient, d, which is a non-dimensional parameter that is calculated as

$$d = J_{\theta Jmax}/J \tag{10}$$

The directionally coefficient accounts for directional spreading of systems and misalignment between multiple wave systems.

A scatter table indicating the expected annual occurrence of sea states is given in Figure 3. Sea states are sorted by H_{m0} and T_e, and the bin widths are 0.5 m and 1 s respectively. A similar table is given in Figure 4, but here the expected annual contribution to incident wave energy of each H_{m0}-T_e sea state is indicated. The contribution to annual wave energy for a given bin was calculated as the sum of the J values of sea states sorted to that bin, multiplied by the one hour window accounted for by each sea state. The sea state with the greatest occurrence occurs at 1.5 m and 7 s, whereas the sea state with the greatest contribution to annual wave energy occurs at 2.0 m and 7 s. Most of the occurrences, and most of the incident wave energy, are accounted for by a fairly narrow subset of H_{m0}-T_e sea states.

A wave rose indicating expected annual occurrence for H_{m0}-θ_{Jmax} sea states is given in Figure 5. An indication of occurrence for each directional bin regardless of H_{m0} is given in Figure 6. It can be seen that while the greatest number of seas arrive from the northeast, a significant portion also arrive from the north.

The expected directional distribution of the H_{m0}-T_e sea states, as θ_{Jmax} and d, are indicated in Figures 7 and 8, respectively. The mean value of θ_{Jmax} over H_{m0}-T_e space shows a very clear pattern as expected, with the long period swell seas coming from the north and the steeper wind seas coming from the northeast. The mean directionality coefficients also exhibited a pattern, with the swell dominated seas being nearly unidirectional and the wind dominated seas being somewhat more directionally spread. It is of interest to compare the directionality coefficient to the cos-2s spreading index. Assuming all wave components have identical mean directions and spreading indices, the directionality coefficient was calculated for the directional distribution resulting from various spreading index values. According to section 3.5.8.7 of [3] wind seas typically have a spreading index between 4 and 9, while swell tends to have a spreading index of 13 or greater. This corresponds to wind seas with directionality coefficients ranging from 0.80 to 0.90, and swell with $d \geq 0.93$. These typical ranges match up quite nicely with the mean values depicted in Figure 8.

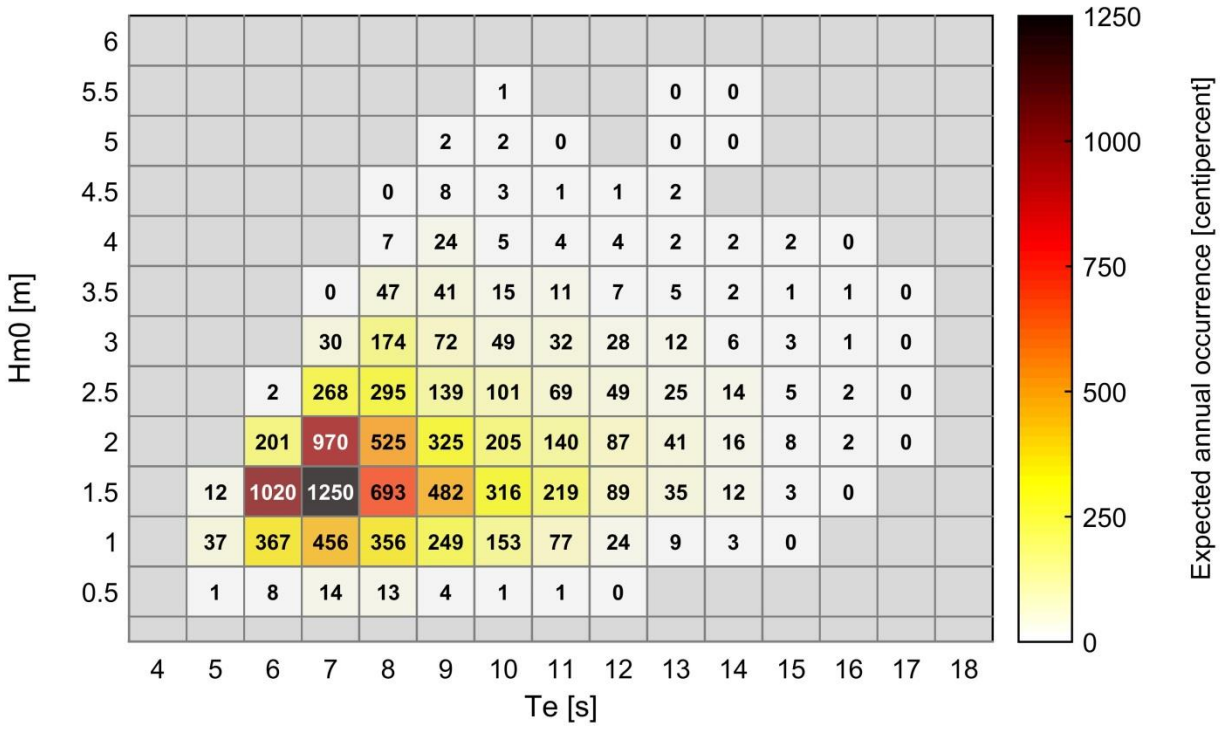

Figure 3 – Expected annual occurrence of H_{m0}-T_e sea states.

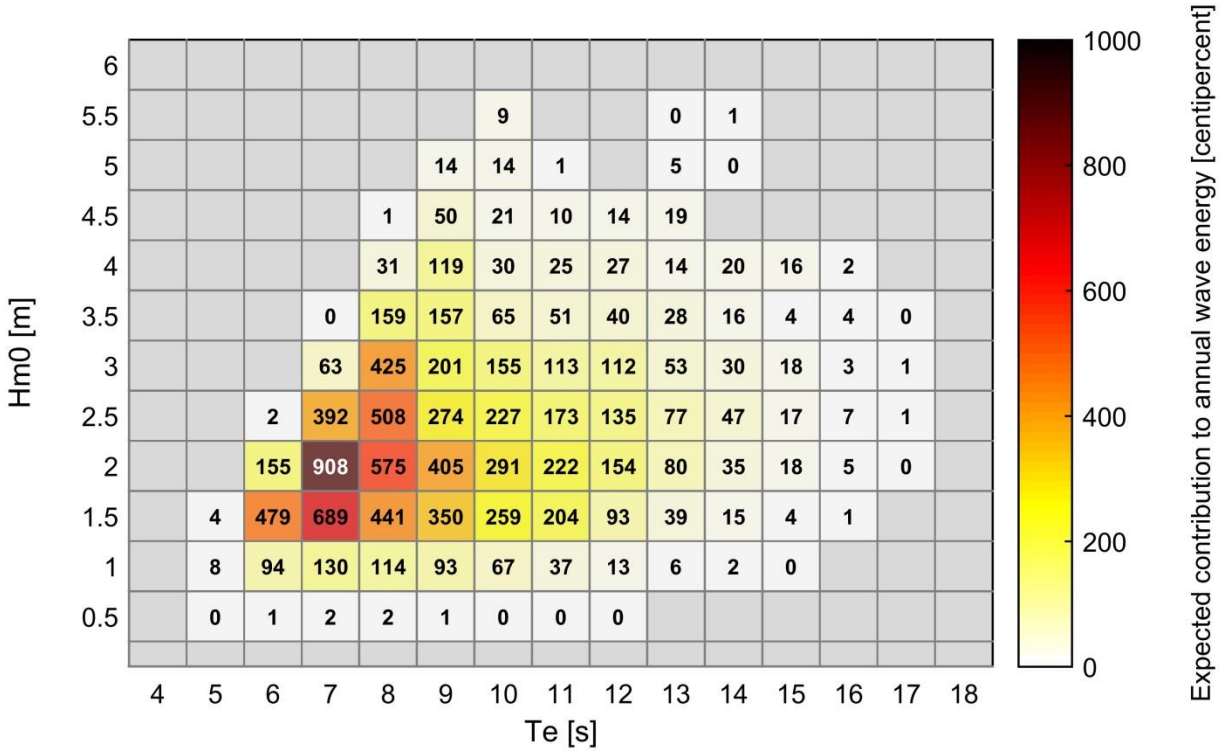

Figure 4 – Expected contribution to annual wave energy of H_{m0}-T_e sea states.

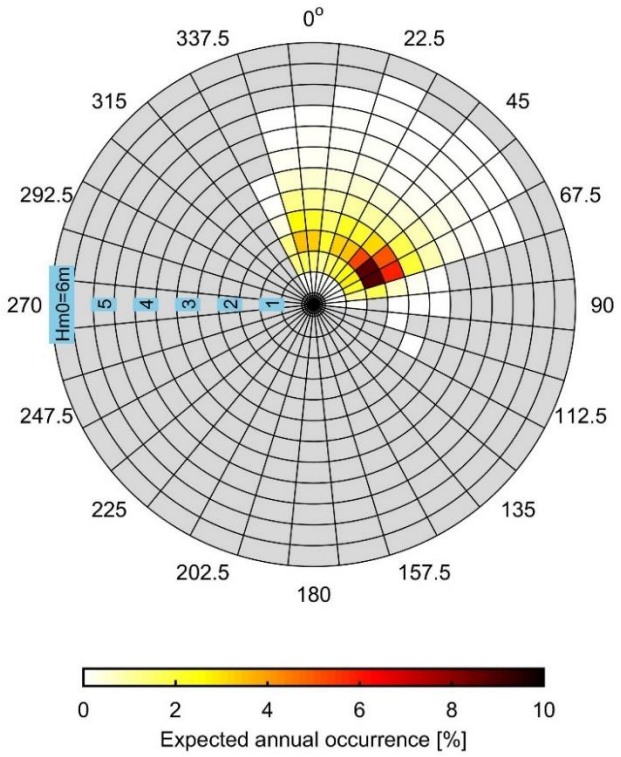

Figure 5 – Wave rose of expected annual occurrence of H_{m0}-θ_{Jmax} sea states.

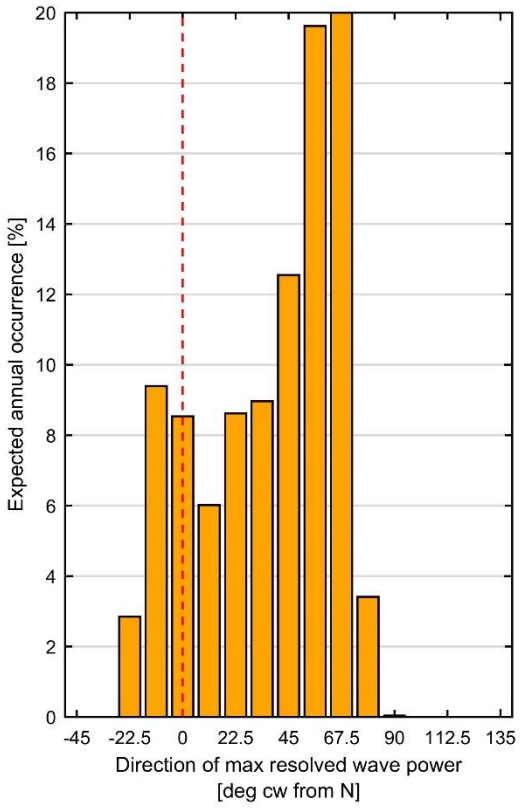

Figure 6 – Expected annual occurrence for seas characterized by θ_{Jmax}.

The mean spectral width of the H_{m0}-T_e sea states is depicted in Figure 9. It may be illustrative to point out that a JONSWAP spectrum with a peak enhancement factor of 1 (i.e. Pierson-Moskowitz) has an ϵ_0 of 0.281 and with a peak enhancement factor of 3.3 it has an ϵ_0 of 0.231; for a very narrow spectrum ϵ_0 tends towards zero. Indeed the values in Figure 9 indicate mean spectra that are broader than a PM spectrum, suggesting that the wave conditions may be better represented by the observed spectra than by a theoretical shape.

Mean one-dimensional frequency spectra were calculated for each H_{m0}-T_e bin. By way of example, mean observed spectra along with their fitted spectra are shown in Figure 10 for two commonly occurring H_{m0}-T_e sea states. Figure 11 indicates the number of samples available for each H_{m0}-T_e bin, as well as the H_{m0} and T_e of each of the mean spectra. Generally speaking, the H_{m0} and T_e of the mean spectra do not coincide with the center of the bin; this is another reason to suggest using the unscaled observed mean spectra to represent the operational sea states. Indicated in Figure 11 by slightly larger dots with cyan faces are the 42 most commonly occurring H_{m0}-T_e bins, which account for 98% of the occurrences.

Empirical cumulative distribution functions for six key wave parameters are shown in Figure 12, and the 1st and 99th percentiles are indicated. We see that 98% of individual sea states observed in the modeled data set have an H_{m0} between 0.8 and 3.6 m, and a T_e between 5.6 and 13.3 s. Furthermore, 98% of sea states have a spectral width between 0.25 and 0.55, and a significant steepness between 0.01 and 0.057 (equivalent to a range of 1/100 to 1/18). Finally, 98% of sea states have a θ_{Jmax} between -19 and 77° with a directionality coefficient between 0.62 and 0.96 (equivalent to a range of cos-2s spreading indices of 1.4 to 24, following the assumptions outlined previously).

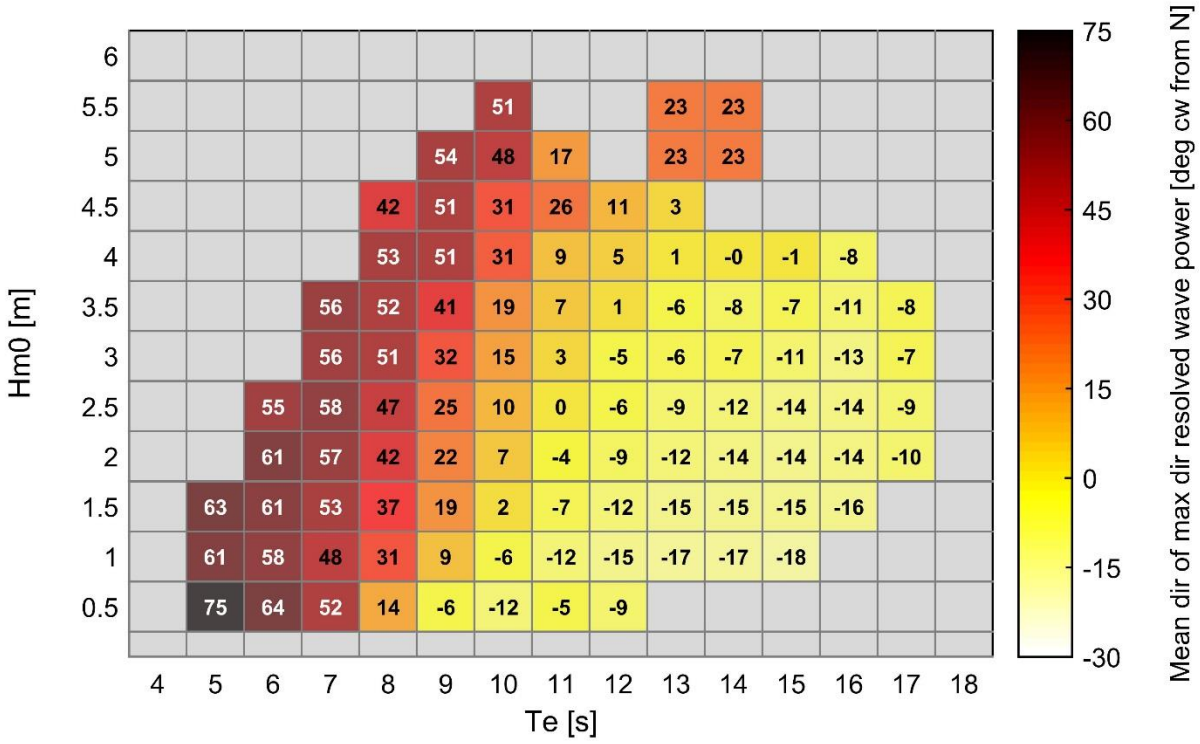

Figure 7 – Mean θ_{Jmax} for H_{m0}-T_e sea states.

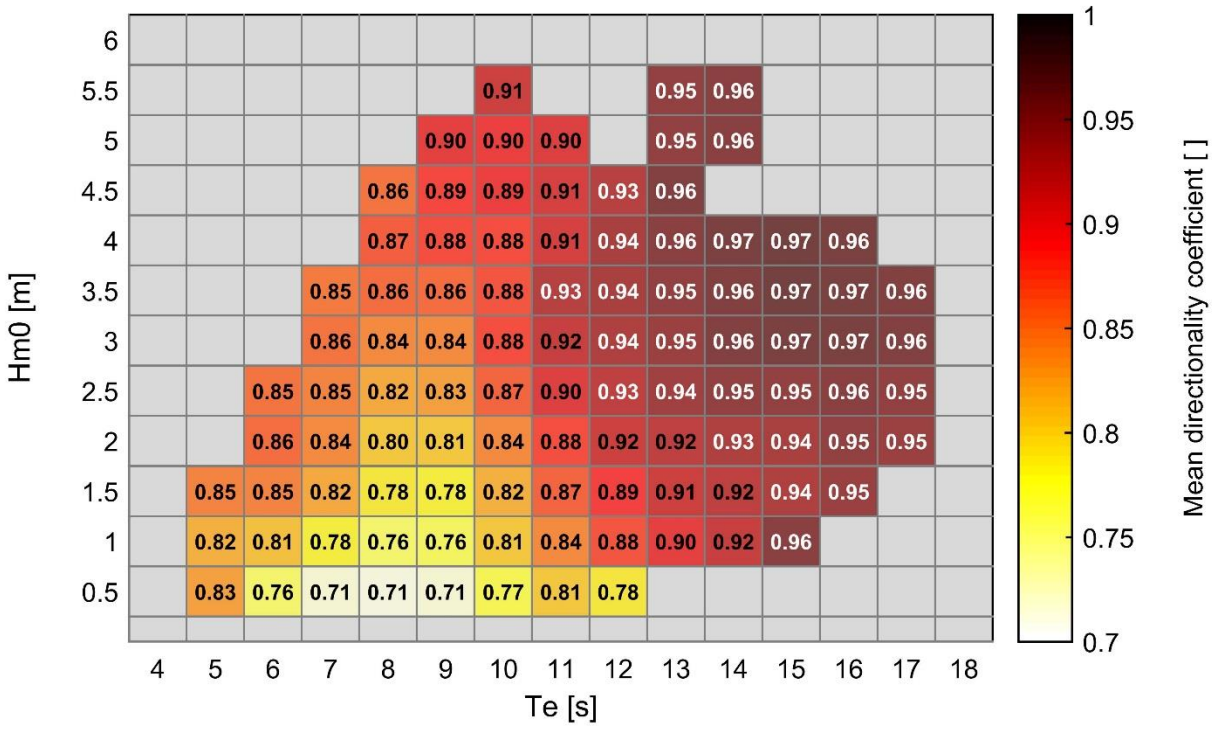

Figure 8 – Mean directionality coefficient for H_{m0}-T_e sea states.

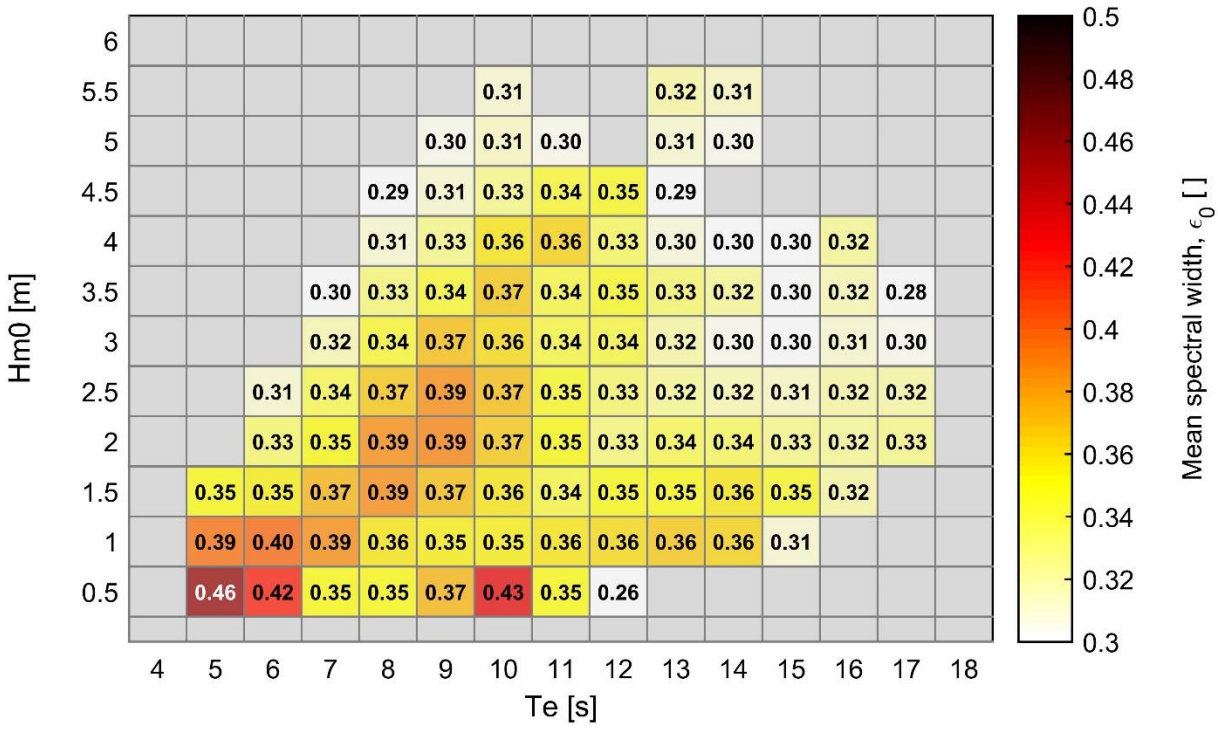

Figure 9 – Mean spectral width for H_{m0}-T_e sea states.

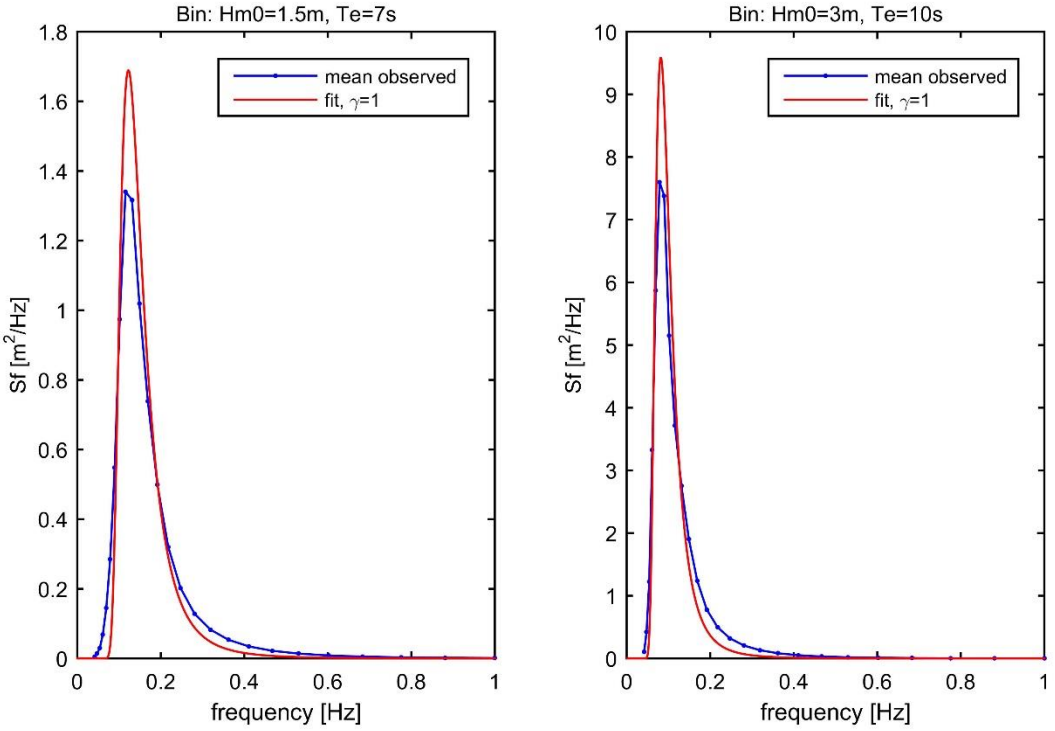

Figure 10 – Comparison of mean observed spectra and fitted JONSWAP spectra.

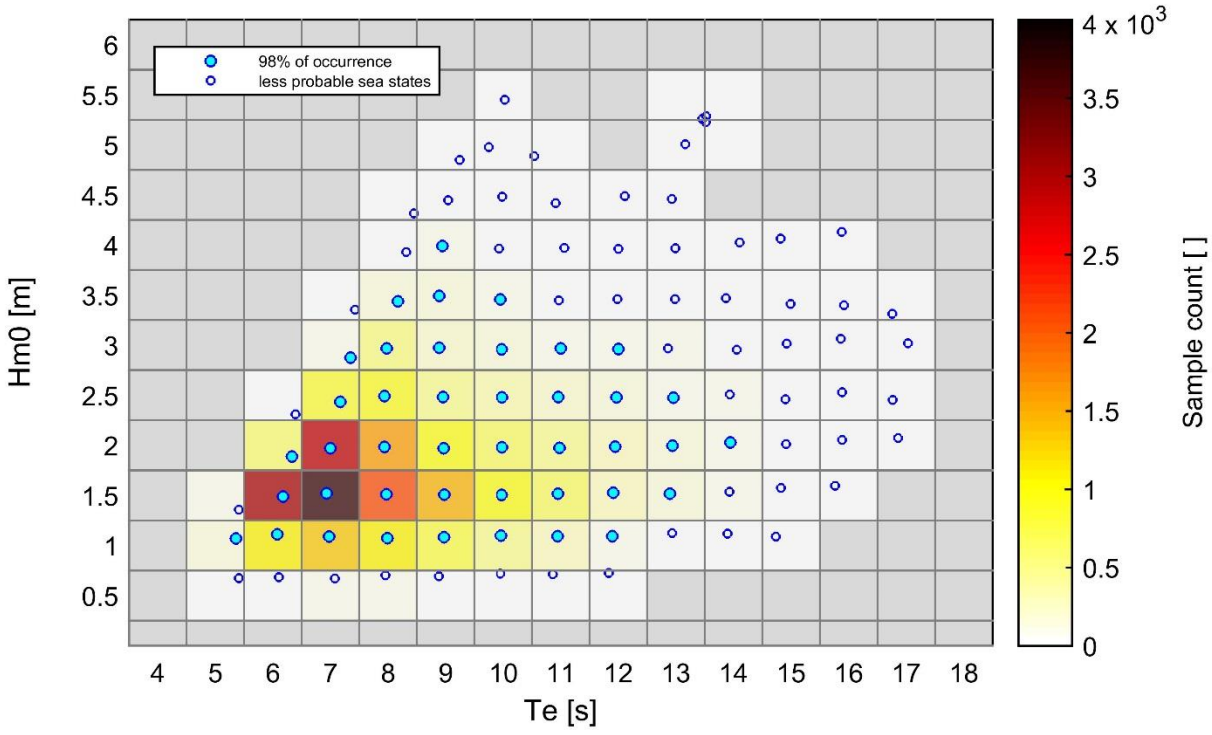

Figure 11 – Sample counts for 34 year data set, with location of H_{m0} and T_e of mean spectra.

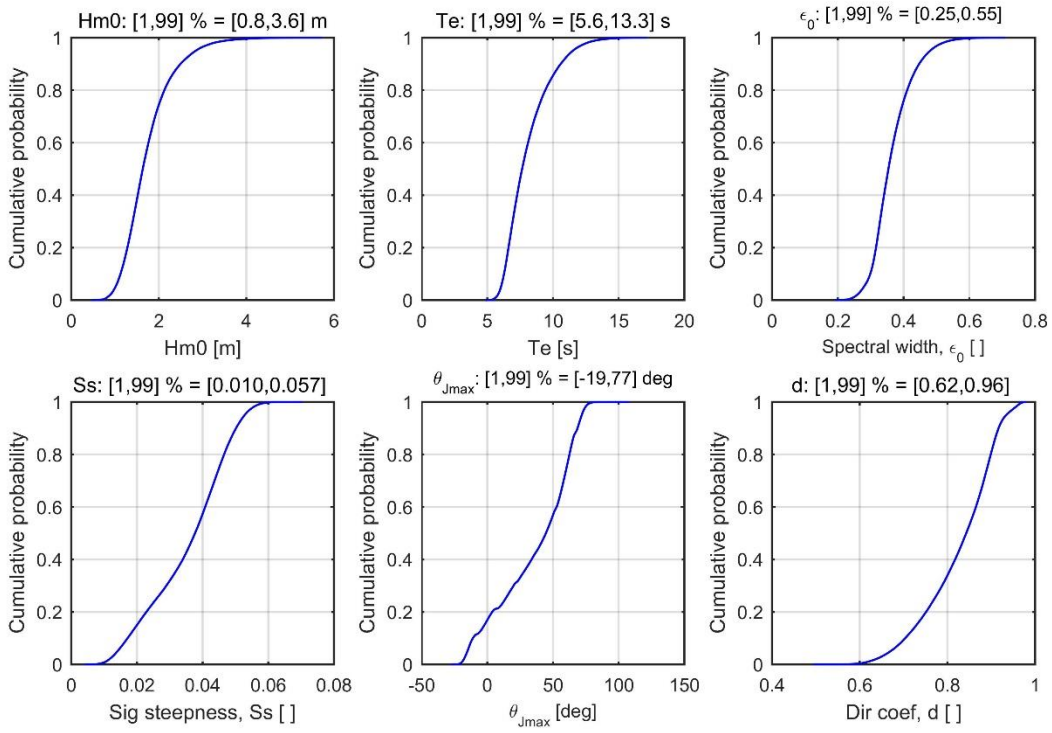

Figure 12 – Empirical CDFs for six key sea state parameters.

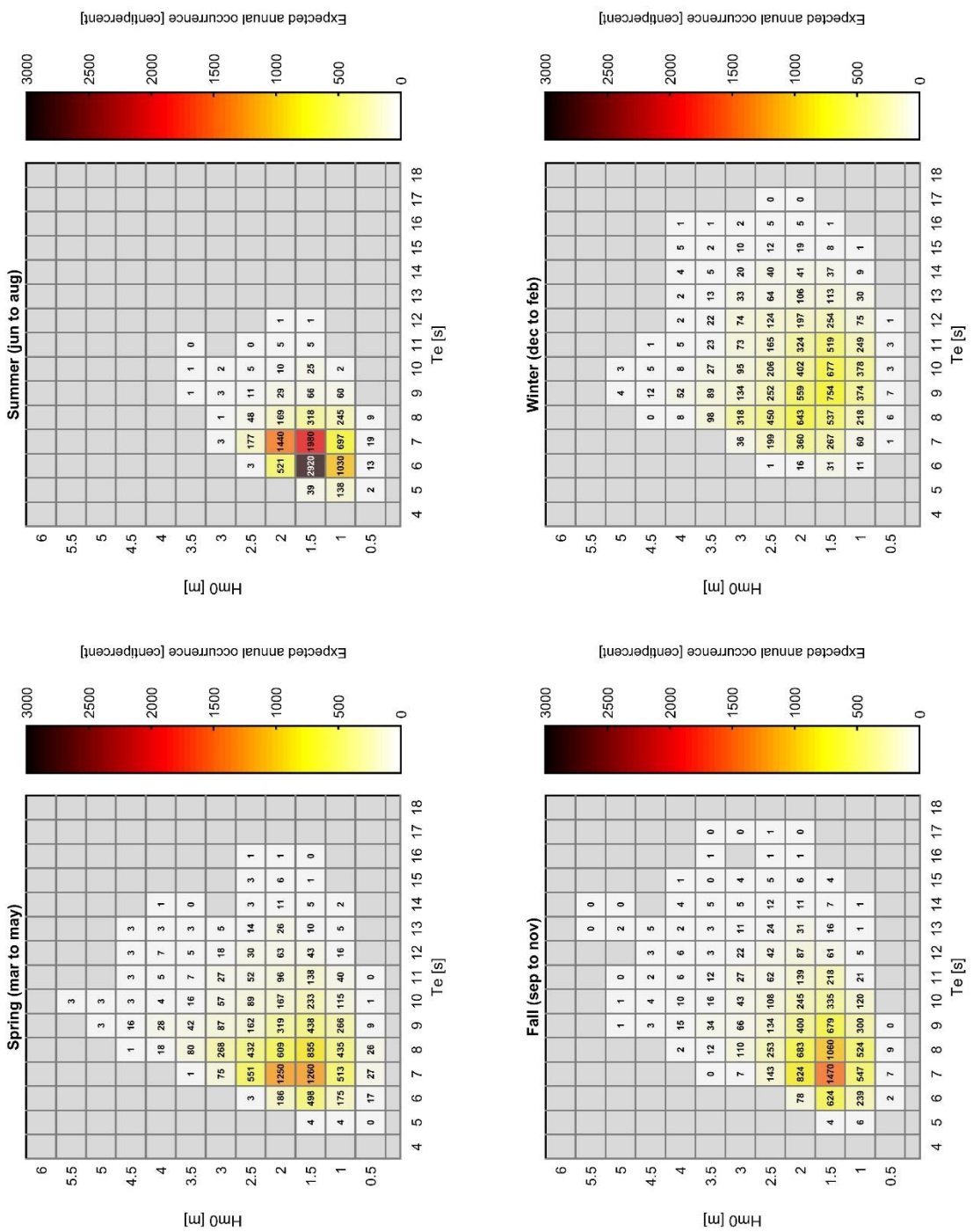

Figure 13 – Expected annual occurrence of H_{m0}-T_e sea states, by the seasons.

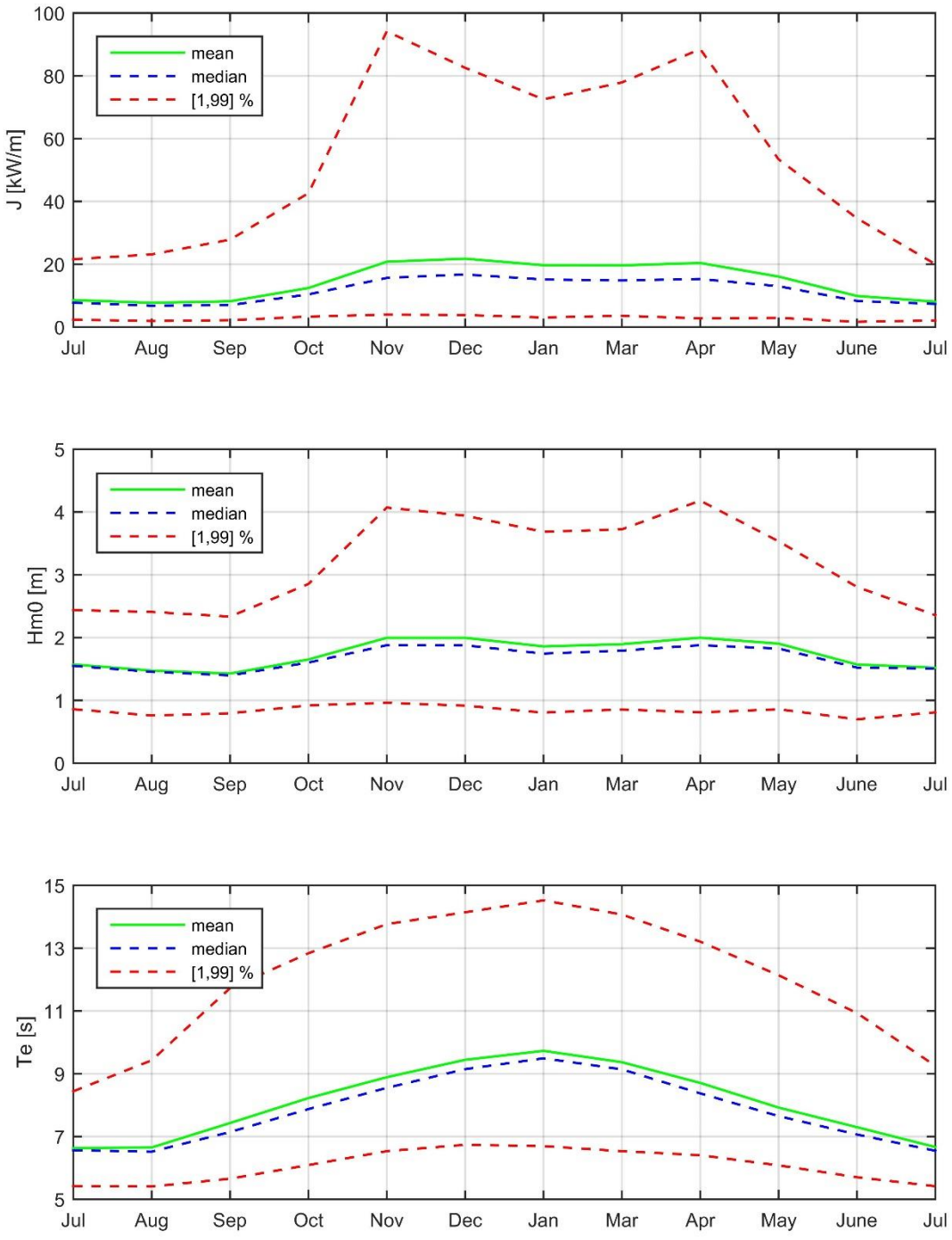

Figure 14 – Monthly expectations and statistical ranges for J, H_{m0} and T_e.

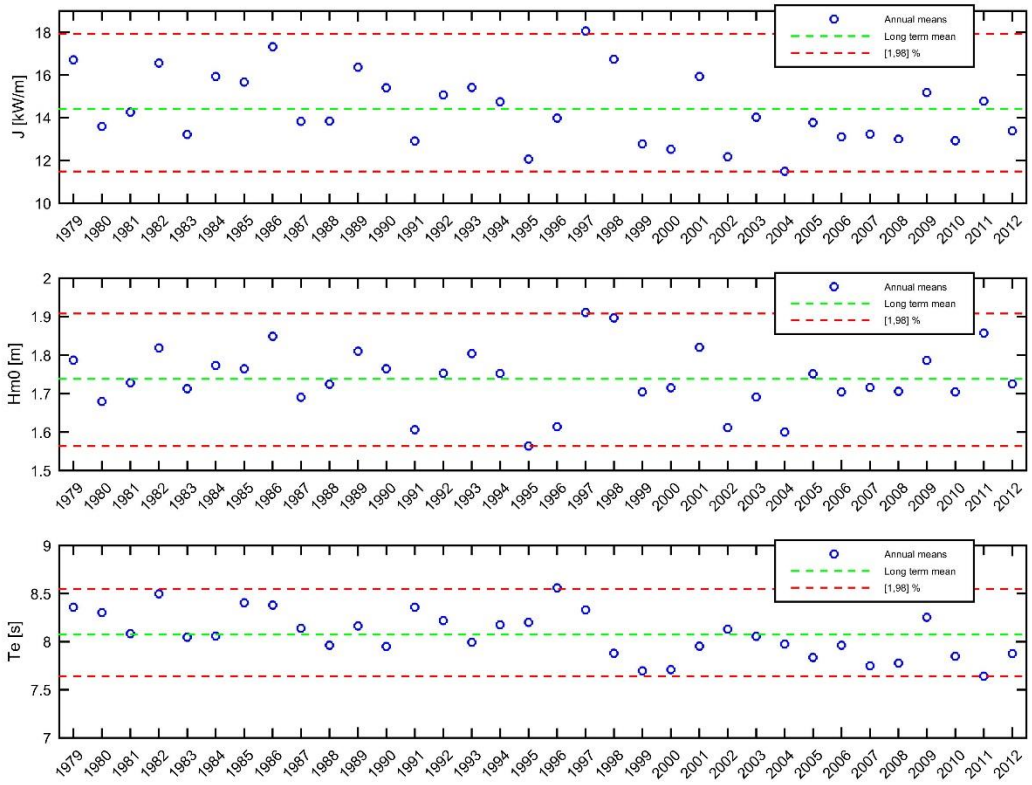

Figure 15 – Annual variability of J, H_{m0}, and T_e.

To illustrate expectations of seasonal changes in wave conditions, Figure 13 depicts scatter tables of expected annual occurrence for each of four distinct seasons. It is seen that in the summer the sea states are tightly focused in the range of 6 to 8 s in energy period, whereas in the winter the sea states are broadly distributed over the range of 7 to 12 s in energy period. Figure 14 depicts the monthly mean and median values of J, H_{m0} and T_e, along with the 1st and 99th percentiles. The seasonal shifts are obvious, with wave power, wave height and wave period all at their greatest over the winter months and at their lowest over the summer months. Interestingly, while median Hm0 and J are fairly consistent from November to April, the peaks occur at the shoulders rather than in the middle of winter. Median H_{m0} is roughly 2m from November to May, and down to roughly 1.5 m from June to September. The annual variability of these same three parameters is depicted in Figure 15. Assuming an expected variability of over the range of the 1st and 99th percentiles of the 34 annual means, we would expect annual average J to fall between 11.5 and 18 kW/m which will have a significant influence on the energy extracted by the WEC over the course of the testing at WETS.

An important aspect of the wave conditions is the expected occurrence of weather windows that allow for operations such as transport, deployment, recovery and maintenance. The expected occurrence annually of sea states in which H_{m0} is at or below a specified threshold value, for at least a specified number of hours, is given in Figure 16. The values indicated in this figure represent the ratio of the total number of sea states in the dataset that fit the criterion, to the the total number of sea states in the dataset. While this information is useful, it does not speak to the distribution thoughout the year. To aid in operational planning, the liklihood of a given weather window occurring within a specified period of time was analyzed throughout the year. A period of two weeks was selected for the plots included here as Figure 17.

Clearly, if an operation can be performed in less time or in more energetic seas, the probability of a suitable weather window occuring over a reasonable time horizon increases. Furthermore, it is clear that operations that can be scheduled should be scheduled for the summer months (roughly June to September). Note that wave period was not considered in this analysis, though it is assumed that most operations will tolerate a larger Hm0 if the sea state is less steep. When operations planning enters a more detailed stage, a more nuanced analysis of weather windows will be performed.

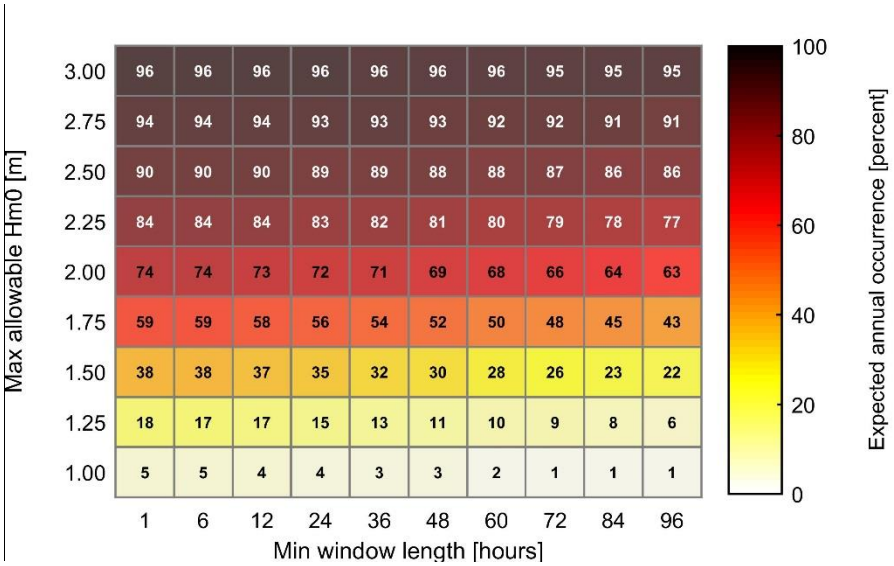

Figure 16 – Expected annual occurrence of specified weather windows.

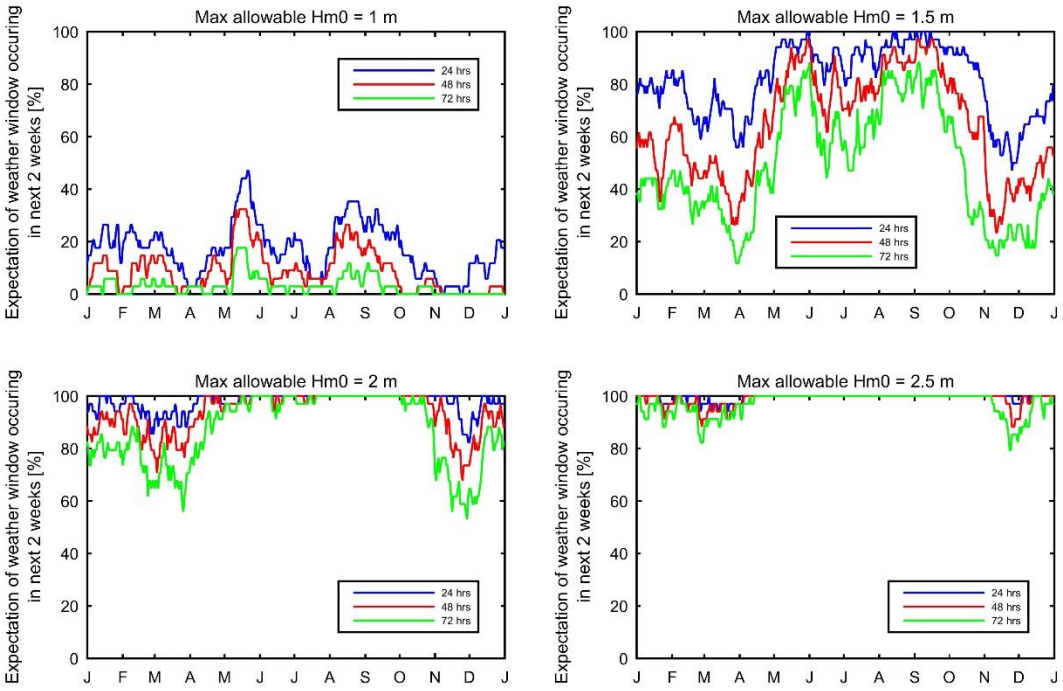

Figure 17 – Expectations of specified weather windows throughout the year.

2.3 Extreme Seas

H_{m0} associated with R-year return seas is derived from the 13 year dataset measured at CDIP 098. Peaks Over Threshold (POT) is used, as DNV [3] recommends using an event based model such as POT where seas are relatively calm much of the time but are punctuated by infrequent, intense events. DNV further recommends fitting the threshold excesses to either an exponential distribution or a two-parameter Weibull distribution; there is also a specific recommendation against using a general Pareto distribution. The exponential distribution was chosen for this study as it yielded a more stable result. A separation period of 72 hours was selected, to assure independence of the peaks over threshold.

The 50-year return H_{m0} over a range of H_{m0} thresholds is given in Figure 18. A lower threshold decreases statistical uncertainty (by allowing more peaks over threshold) but may reduce the accuracy by included data points that do not belong in the tail of the distribution. It is seen that the estimates are fairly stable with a threshold of roughly 3 m or greater. Based on this sensitivity study, a threshold of 3 m is selected. This threshold retains 205 storm peaks, or roughly 16 storm peaks per year. An exponential distribution is then fit to the 205 threshold excesses using Maximum Likelihood Estimation (using the Matlab function *expfit*), and the fitted distribution is used to estimate H_{m0} associated with a range of return periods at a 95% confidence level (see Figure 19). H_{m0} estimates associated with return periods of 1, 50 and 100 years are given in Table 2. The more conservative, upper limits of the estimates will be used for design purposes.

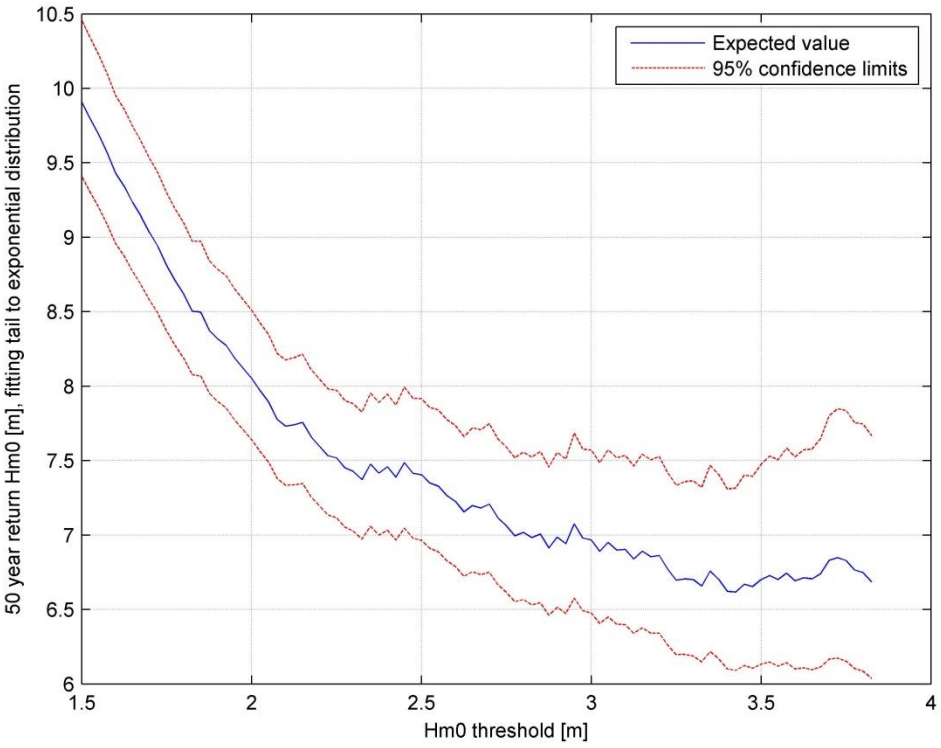

Figure 18 – Stability of extreme seas estimates over a range of H_{m0} thresholds.

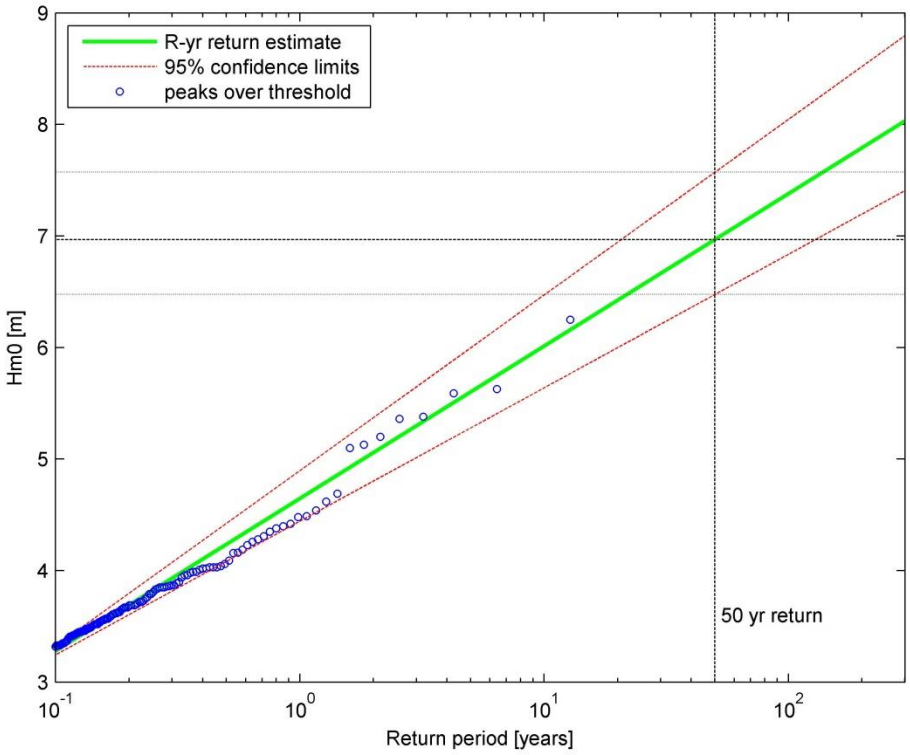

Figure 19 – H_{m0} estimates associated with R-year return seas.

Table 2 – R-year return seas H_{m0} estimates with 95% confidence limits.

	R-year return sea H_{m0} estimates with 95% confidence limits [m]		
Return period [yr]	**Lower limit**	**Expected value**	**Upper limit**
1	4.44	4.65	4.90
50	6.48	7.00	7.57
100	6.84	7.38	8.04

Due to the open ocean conditions (long fetch and deep water), a JONSWAP spectrum with a peak enhancement factor (γ) of 1 is assumed (i.e. Pierson-Moskowitz spectrum). Indeed, examination of the modeled data set spectra in the steepest of the large H_{m0} bins (H_{m0} = 5.5 m and T_e = 10 s, called 5510) show a reasonably good fit to γ = 1, adding confidence to the decision to use a PM spectrum. Furthermore, the spectra in bin 5510 have significant steepness values ranging from 1/18 to 1/16 (S_s of 1.16 is exceeded in only 0.015% of the 34 year data set). Given a S_s value, the average zero-crossing period, T_z, can be calculated using equation (6). For a JONSWAP spectrum with a γ of 1, the relationship between characteristic periods of interest are $T_e = 1.209\ T_z$ and $T_p = 1.408\ T_z$. Thus for the upper limit of the 50-year return significant wave height, H_{m0_50yr}, we will assume an associated T_{e_50yr} of between 10.6 and 11.3 s for this range of S_s values. The upper limit R-year return seas H_{m0} estimates that will be used for design purposes, along with other associated parameter estimations, are given in Table 3. Although parametric sea states are listed for return periods of 1, 50 and 100 years, the data and methodology presented here allows for parametric representations for other return periods as well.

Table 3 – R-year return seas estimates for design.

		Return period [yr]		
Parameter	**Units**	**1**	**50**	**100**
H_{m0}	m	4.90	7.57	8.04
γ	-	1	1	1
S_s	-	1/18 to 1/16	1/18 to 1/16	1/18 to 1/16
T_e	s	9.09 to 8.57	11.3 to 10.6	11.6 to 11.0
θ_{Jmax}	°	-19 to 77	-19 to 77	-19 to 77
d	-	0.9 to 1.0	0.9 to 1.0	0.9 to 1.0
cos-2s index	-	≥ 9	≥ 9	≥ 9
T_{ass}	m	7.75 to 9.96	9.65 to 12.4	9.92 to 12.8
H_{max}	s	8.59 to 8.41	13.1 to 12.8	13.8 to 13.5

The characteristic direction, $\theta_{Jmax,}$ of the design seas will be assumed to fall anywhere within the range observed in central 98% of the modeled data set (see Figure 12). While the seas in bin 5510 all have θ_{Jmax} near 50°, they all come from the same storm and so it is reasonable to assume that the design sea could come from a wider range of directions. The expected value of the directionality coefficient is taken from Figure 7; however, a more conservative design may come from an assumption of a unidirectional sea state and so d from 0.9 to 1.0 may be considered in design.

Although the dynamic and resonant nature of the WEC response suggests that a simulation in stochastic seas will give a more realistic result than in deterministic seas (i.e. regular wave), it is unclear at this point if a stochastic analysis is technically feasible. As such, estimates of individual design waves will also be given. Following 1.D.3.2 of [2], the maximum individual wave height, H_{max}, and associated period, T_{ass}, are calculated as

$$3.5\sqrt{H_{m0}} < T_{ass} < 4.5\sqrt{H_{m0}} \tag{11}$$

$$H_{max} = H_{m0}\sqrt{0.5\ \ln\left(\frac{3600\ \text{s}}{T_{ass}}\right)} \tag{12}$$

Note that this methodology is specifically intended to be applied to deep water waves, which satisfy the condition $d/(gT^2) > 0.06$ where d is the water depth. For the 80 m test site this condition is technically violated for $T > 11.7$ s. The upper end of the T_{ass} range for 50- and 100-year return seas marginally violates the deep water condition; CPwr assumes that for these marginally intermediate depth waves the methodology employed remains suitable.

No direct observational evidence of the prevalence of breaking waves at the test site was located. However, by making the conservative assumption of unidirectional waves and furthermore by characterizing a sea state by a single design wave the guidance on breaking waves presented in 3.4.6 of [3] can be followed, in which the breaking wave height limit, H_b, is calculated as

$$H_b = 0.142\ \lambda \tanh\frac{2\pi h}{\lambda} \tag{13}$$

where λ is the wave length corresponding to T_{ass} and water depth, h. The lower limit of T_{ass} from equation (11) is used as the steeper wave is more likely to break. A sea state length of 3 hours is used in conjunction with equation (12) to calculate H_{max}. Figure 20 depicts H_{max} and H_b as a function of H_{m0}, and shows that breaking waves are not expected at the test site.

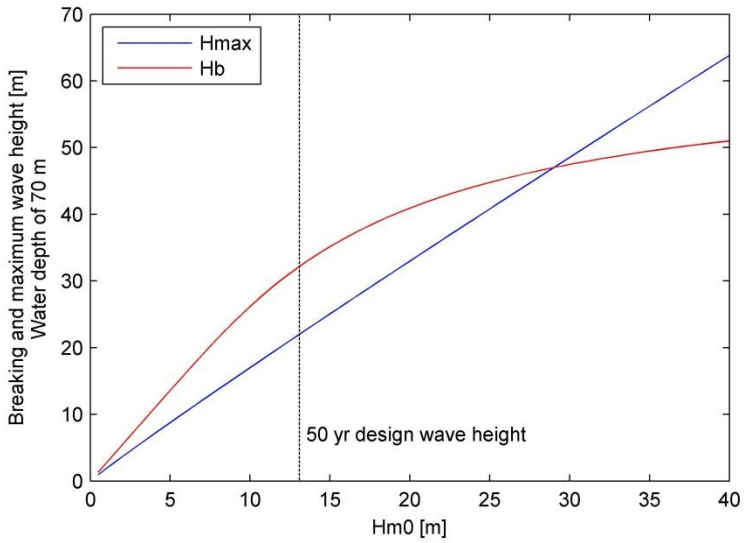

Figure 20 – Maximum expected wave height and breaking wave limit.

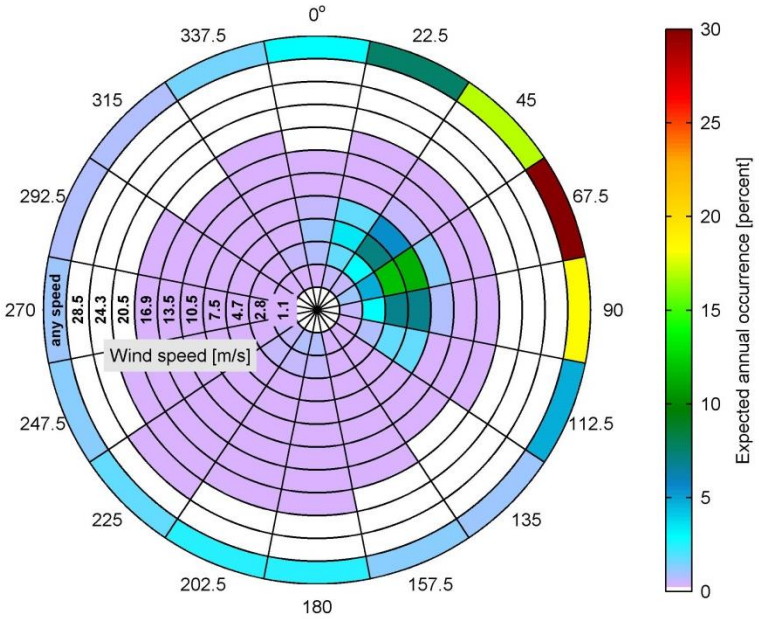

Figure 21 – Wind rose of expected annual occurrences.

3 WIND

The following characterization of design wind speed at the test site was provided by WETS [9]. Annual and monthly summaries of winds based on hourly observations and monthly peak gusts observed at Kaneohe Bay Marine Corps Air Station (21°27'N,157°47'W) are available as the International Station Meteorological Climate Summary (1996), jointly produced by Fleet Numerical Meteorology and Oceanography Detachment, National Climatic Data Center and USAFETAC OL-A. The summary is based on observations over the period of 1945 to 1995. The reference height for the reported wind speeds is 6 m. Over 70% of observed winds are trade winds, from a sector bounded by the northeast and the east-southeast,

with an average speed of 5 m/s. A wind rose is presented in Figure 21. Assuming a mean observed air temperature of 23.5 °C (see section 7), the air density is interpolated from appendix F of [3] as 1.216 kg/m^3.

The referenced report [9] describes the fitting of a Gumbel distribution to 36 annual maximum gusts, and the resulting R-year return estimates for sustained (1 minute and 10 minute) and gust (3 second) wind speed. The reported gusts are assumed to be 3 second wind speeds, and the 1- and 10-minute wind speeds are calculated using a methodology presented in the Shore Protection Manual (1984). The results are converted from the reference height of 6 m to a reference height of 10 m, following the equation presented in section 2.3.2.11 of [3] (rearranged here)

$$U_{10} = \frac{U_y}{1 + 0.137 \ln\left(\frac{y}{y_{10}}\right)} = 1.075\, U_y \tag{14}$$

where U_{10} is the wind speed at the reference height of 10 m, U_y is the wind speed at a reference height of y, and y_{10} is equal to 10 m. The results thus converted to a 10 m reference height are summarized in Table 4. Note that the referenced report provided wind speed estimates for return periods up to 25 years; the wind speeds reported here for a 50 year return period are extrapolated from these results. Furthermore, 1-hr sustained wind speeds are estimated following 2.3.2.11 of [3] (rearranged here)

$$\begin{aligned} U_{60\text{min},10\text{m}} &= U_{10\text{min},10\text{m}}\left(1 - 0.047 \ln\left(\frac{60\text{ min}}{10\text{ min}}\right)\right. \\ &= 0.9158\, U_{10\text{min},10\text{m}} \end{aligned} \tag{15}$$

Table 4 – R-year return wind speed estimates, at a reference height of 10 m.

	R-yr return wind speed estimates [m/s]			
Return period [yr]	3-sec gust	1-min sustained	10-min sustained	1-hr sustained
2	25.5	21.0	16.9	15.5
5	32.1	26.4	21.3	19.5
10	36.8	30.3	24.3	22.2
25	42.5	34.9	28.1	25.7
50	46.4	38.2	30.7	28.1

Although the vast majority of the winds come from the northeast (see Figure 21), winds are observed from all directions and indeed the extreme wind speed events are observed to come from a sector bounded by the south and the west-southwest. For design purposes the wind shall be assumed to come from the direction leading to the most conservative loading.

4 CURRENT

No long term current data could be located for the test site. The following information is taken from an Environmental Assessment report [10] prepared by the Office of Naval Research for the original 30 m test site at WETS.

The currents around Hawaii are influenced by the semi-diurnal tide, the large-scale oceanic current and the wind. The tide is the dominant influence in most areas around the Hawaiian Islands and there is no evidence to suggest that the WETS site is an exception. According to the referenced report, all current measurements around Oahu prior to 1978 were summarized in the *Circulation Atlas of Oahu, Hawaii* (Bathen, 1978), and this atlas indicates for the test site reversing currents flowing parallel to the bathymetric contours, with flood and ebb currents moving towards the east and west respectively. Maximum predicted current speeds

of 0.62 and 0.51 m/s (1.2 and 1.0 kn) for flood and ebb currents, respectively, were reported. Typical tidal current speeds of 0.26 m/s (0.5 kn) are reported. These current speeds are assumed to be at the surface; current speed profiles are discussed below.

Wind induced currents are estimated using the 1-hr sustained wind speed, as specified in 4.1.4.4 of [3] under the assumptions of deep water and long fetch

$$v_{c,wind}(0) = 0.015\, U_{60\text{min},10\text{m}} \tag{16}$$

where $v_{c,wind}(0)$ is the wind induced current speed at the sea surface and $U_{60\text{min},10\text{m}}$ is the 60-min sustained wind speed at a 10 m height.

The total current will be assumed to be the sum of the tidal and wind current components. It will be assumed that the wind and tidal currents are parallel to one another, as this will yield the highest current speed and the most conservative loading scenario. The tidal current will be assumed to decay following a power law, and the wind current will be assumed to decay linearly and vanish at a depth of 50 m (following 4.1.4 of [3]) such that

$$v_{c,tide}(z) = v_{c,tide}(0)\left(\frac{h+z}{h}\right)^{\alpha} \quad \text{for } z \le 0 \tag{17}$$

$$v_{c,wind}(z) = v_{c,wind}(0)\left(\frac{h_0+z}{h_0}\right) \quad \text{for } -h_0 \le z \le 0 \tag{18}$$

where v_c is the current velocity as a function of depth, z is the distance from the still water surface positive upwards, h is the water depth (positive, still water level), α is assumed equal to 1/7 and h_0 is assumed to be 50 m.

Proposed values for surface current speeds, from tidal and wind sources, are summarized Table 5.

Table 5 – Representative current speeds at the sea surface.

	Surface current speed estimate [m/s]	
Current component	Typical (2-yr return)	Extreme (50-yr return)
Wind	0.23	0.42
Tidal	0.26	0.62

5 TIDE

The tides in Hawaii are semi-diurnal. The tidal datums presented below are taken from the nearby tidal station ID 1612480 (Mokuoloe, HI), obtained from the National Oceanic and Atmospheric Administration's (NOAA) website (www.tidesandcurrents.noaa.gov). This station is located at 21°25.9' N and 157°47.4' W. The tidal datum analysis period covers the period of 1983 to 2001. The mean tidal range is reported as 0.453 m and the maximum astronomical tidal range is reported as 1.13 m. The tidal datums are summarized below in Table 6.

The depths given elsewhere (e.g. Table 1) are mean lower-low water, and the same relationships are expected at the test berths as at the tidal station. Thus the highest and lowest astronomical tides at any of the test site locations will be, respectively, 0.89 m above and 0.24 m below the stated mean lower-low water elevation. For example, at the center of Berth B where the mean lower-low water is 80 m the astronomical tidal range will have depths of 80.89 and 79.76 m.

Table 6 – Tidal datums.

Mean Sea Level	1.210 m
Mean Higher-High Water	1.536 m
Mean Lower-Low Water	0.890 m
Highest Astronomical Tide	1.778 m
Lowest Astronomical Tide	0.647 m
Highest Sea Water Level	1.981 m
Lowest Sea Water Level	0.457 m

6 BATHYMETRY AND BOTTOM CONDITIONS

Test site bathymetry and a description of the bottom conditions were provided by WETS [11]. A multi-beam bathymetry survey was performed by Sea Engineering and Solmar Hydrographics. The bathymetry in the vicinity of the two test berths, and shoreward, is given in Figure 22. A geophysical sub-bottom profiling was performed by Sea Engineering. This profiling revealed a reef limestone hard bottom, punctuated by a series of terraces. Sediment, primarily sand, covers much of the terraced, hard bottom of the test site seaward of the 50 m contour. Sediment thickness is given in Figure 23. Note that sediment thickness of roughly 10 to 15 m is indicated in the vicinity of the test berths.

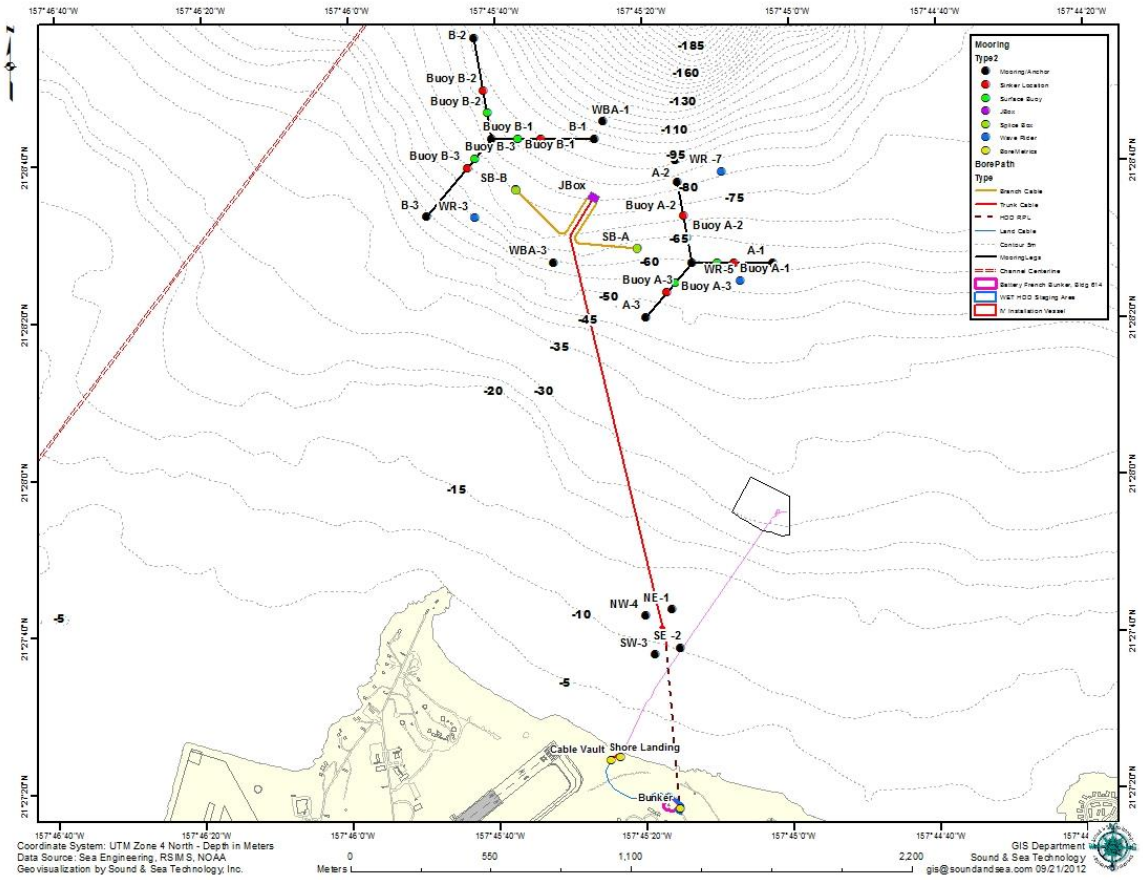

Figure 22 – Test site bathymetry, with proposed offshore cable routing.

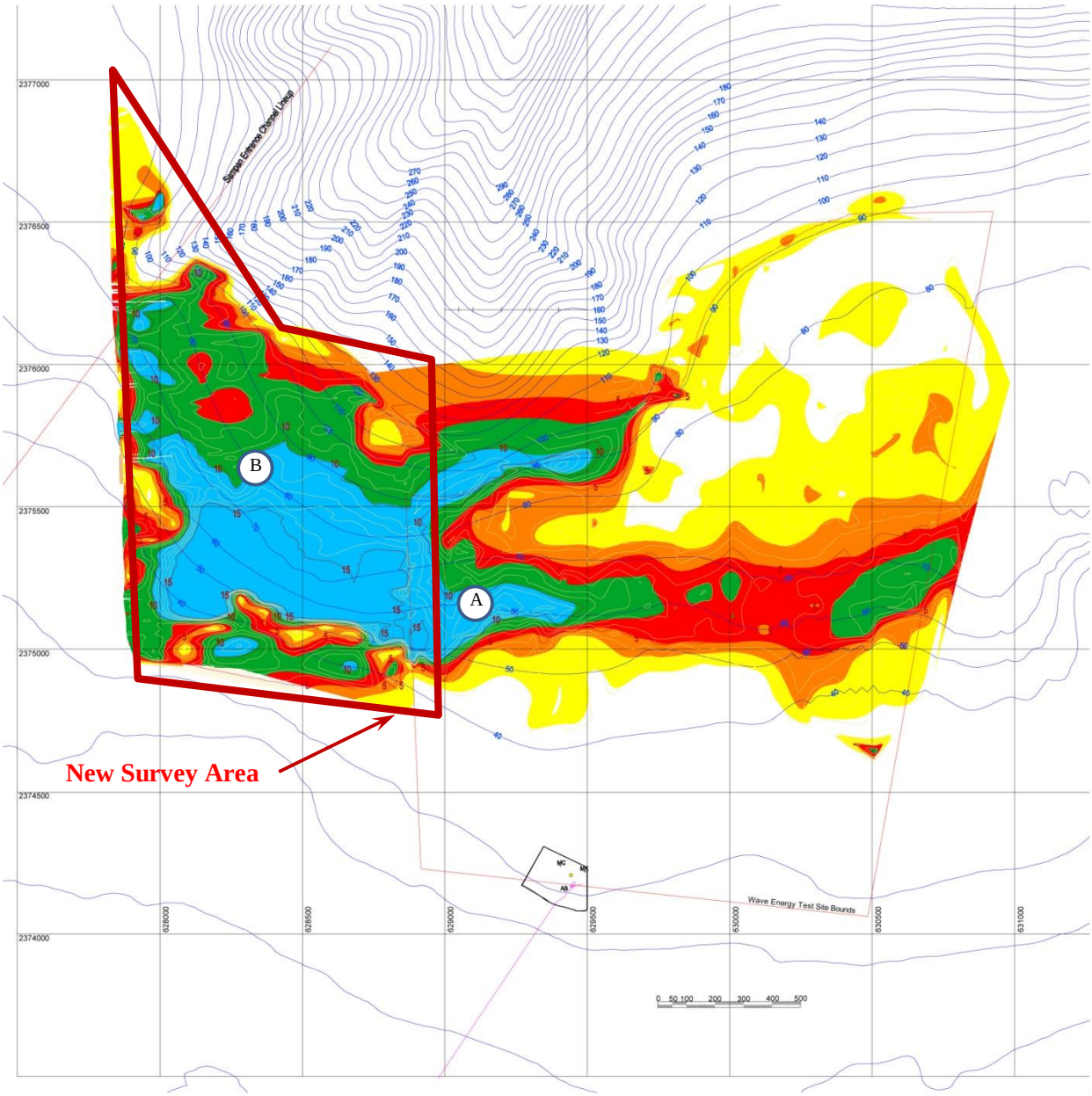

Figure 23 – Sediment thickness at test site.

7 SEISMIC ACTIVITY

There is no expectation of seismic activity at WETS. It is certainly possible for a distant earthquake to send a tsunami to Hawaii (though there are no documented occurrences of a tsunami affecting Kaneohe Bay); however, at the 80 m depth in which the WEC will operate the tsunami would manifest as a very long period, low amplitude wave of no concern.

Earthquakes and tsunamis will be considered to be irrelevant to the design of the StingRAY for deployment at WETS.

8 MARINE GROWTH

No specific guidance has been located regarding marine growth at the WETS test site (or anywhere more generally in the region), however section E 800 of DNV-OS-J101 *Design of Offshore Wind Turbine Structures* (2011) [12] gives guidance on marine growth thickness for several regions. By CPwr's judgment, the most relevant of these regions is offshore of southern California for which it is stated that 'marine growth thicknesses of 200 mm are common'. While it is not made clear at what depth this thickness is commonly observed at, or how much time is required for this growth, this value will be assumed for design purposes. The density of the marine growth shall be assumed to be 1325 kg/m^3 (see B 800 of DnV-OS-E301 *Position Mooring* (2010) [13]).

9 TEMPERATURE

Extreme air temperatures are taken from NOAA's station ID 781 (Kaneohe Mauka, HI), located at 21°25' N and 157°49' W. Records are available over the period of 1949 to 1998. The minimum, maximum and mean air temperatures reported are 12.8, 33.9 and 23.5 °C, respectively.

Extreme sea surface temperatures are taken from CDIP 198, over the same 13 year time period as the wave records. The minimum and maximum sea surface temperatures reported are 22.4 and 28.8 °C, respectively.

REFERENCES

[1] "Certification of Tidal and Wave Energy Converters," Det Norske Veritas, DNV-OSS-312, 2011.

[2] "Offshore Structures: Structural Design," Germanischer Lloyd, GL Rules and Guidelines IV-6-4, 2007.

[3] "Environmental Conditions and Environmental Loads," Det Norske Veritas, DNV-RP-C205, 2010.

[4] J. E. Stopa, J.-F. Filipot, N. Li, K. F. Cheung, Y.-L. Chen, and L. Vega, "Wave energy resources along the Hawaiian Island chain," *Renewable Energy*, vol. 55, pp. 305–321, 2013.

[5] "Comparison of Existing Wave Measurements in the Vicinity of WETS," Columbia Power Technologies, May 2013.

[6] N. Li and K. F. Cheung, "Comparison of Wave Hindcast Model Results with Waverider Measurements: Nov 2012-Oct 2013," Hawaii National Marine Renewable Energy Center, Jan. 2014.

[7] "Wave energy resource assessment and characterization," IEC 62600-101, 2014.

[8] M. J. Tucker and E. Pitt, *Waves in ocean engineering*, vol. 5. Elsevier Science Ltd, 2001.

[9] "Thirty-Meter Test Site Characteristics: WETS Engineering Services Support," Naval Facilities Engineering Service Center, Nov. 2012.

[10] "Environmental Assessment: Proposed Wave Energy Technology Project," Office of Naval Research, Jan. 2003.

[11] "WETS Preliminary Design Report," Naval Facilities Engineering and Expeditionary Warfare Center, Nov. 2012.

[12] "Design of Offshore Wind Turbine Structures," Det Norske Veritas, DNV-OS-J101, May 2014.

[13] "Position Mooring," Det Norske Veritas, DNV-OS-E301, Oct. 2010.

APPENDIX: DIRECTIONAL H_{M0}-T_E SCATTER TABLES

Introduction

The modeled sea state data used to characterize the sea states at the WETS test berth has been sorted by direction and scatter tables produced. The data set consists of hourly spectral records covering a period of 33 years. The sea states were sorted into directional bins of 30° width. For binning the mean direction was used to characterize direction. The sea states were then binned by Hm0 and Te with bin widths of 1m and 1s respectively.

Subsequent sections cover the following:

- Directional parameterization
- Calculation of mean spectra
- Scatter tables
- Data structure

Directional Parameterization

The sea states have now been parameterized using the mean direction (θ_{mean} or MDIR). Previous analysis utilized the direction of maximum directional wave power (θ_{Jmax}); see S1-DB-01 v4.0 Metocean Report for details. The primary difference is that θ_{Jmax} weights directional wave components by the wave power they carry and thus weights more heavily a) components of greater wave height (or variance) and b) components of longer wave period. MDIR on the other hand weights components only by the variance, as

$$MDIR = \text{atan}(S_E/S_N) \tag{1}$$

where

$$S_E = \int_{f,\theta} S_{fd} \sin(\theta)\ df\ d\theta \tag{2}$$

$$S_N = \int_{f,\theta} S_{fd} \cos(\theta)\ df\ d\theta \tag{3}$$

Where S_{fd} is the two-dimensional frequency-directional wave elevation variance density, θ and f are the characteristic values of the directional and frequency bins, and $d\theta$ and df are the widths of the directional and frequency bins.

The change in parameterization is due to an understanding of WEC orientation w.r.t. incident seas based on tank scale observations (see S1-DEL-0021-01 v1.0). In these tests the WEC was observed to weathervane into seas that were initially 45 and 90° off-angle w.r.t. the WEC. A total of five sea states were used, with Hm0 and Te combinations designed to isolate the effect of each. Since the WEC was lightly restrained from weathervaning by the aft tether, the offset from perfect orientation with the waves can be used to assess the tendency of the WEC to orient with seas of varying Hm0 and Te. The conclusion was that the orientation tendency or "weathervaning moment" increased with increasing wave height and, to a lesser extent, with decreasing energy period.

The directional parameter is selected for its utility in predicting the WEC orientation. θ_{Jmax} fails because it more heavily weights longer period seas (as these have proportionally greater wave power) while the

WEC has been observed to favor orientation with shorter periods. MDIR is preferred then because it is only weighted by wave elevation variance. While the periods of the wave components are expected to have an effect, the precise nature of this is not yet understood and so a parameter that ignores period is better than one that is clearly wrong.

An examination of the WETS spectra, even the mean binned spectra, reveal that bimodal sea states are fairly common. Along with clearly bimodal sea states (e.g. directionally distinct sea and swell systems), other asymmetric directional distributions abound. The only tank test data CPwr has is for unimodal, directionally-symmetrical off-angle sea states. While there is data on the WECs response to these off-angle systems, it is not deemed sufficient to estimate the WEC orientation to a complex directional sea state. CPwr proposes that WEC orientation with MDIR is the best assumption.

Scatter Tables

The data set consists of hourly spectral records covering a period of 33 years, for a total of 298,056 records. The sea states were sorted into directional bins of 30° width, with the centers evenly distributed from -75 to 105°. For binning, the mean direction was used to parameter used to characterize direction. The sea states were then binned by Hm0 and Te with bin widths of 1m and 1s respectively.

The following figures depict first the expected annual occurrence in permyriad (i.e. parts per 10,000).

Following the scatter tables is a tabular listing of all sea state bins with a non-zero occurrence.

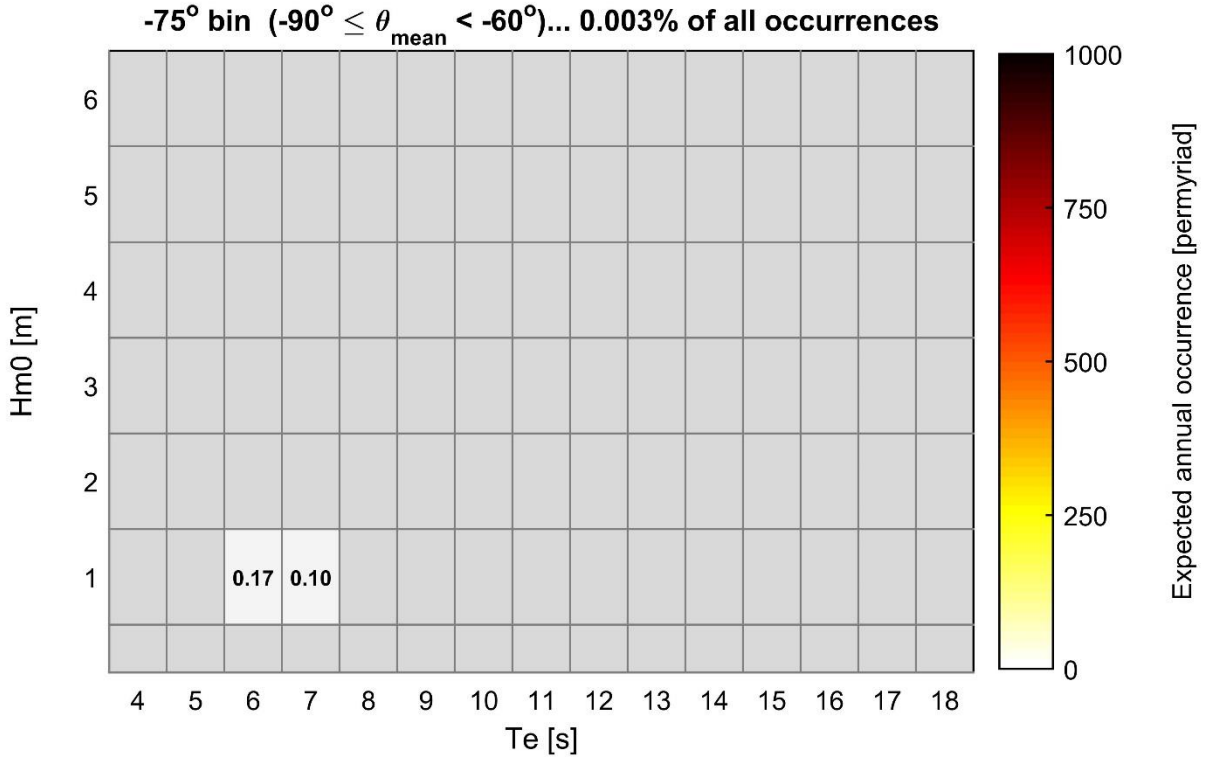

Figure 24 – Occurrence for -75° bin.

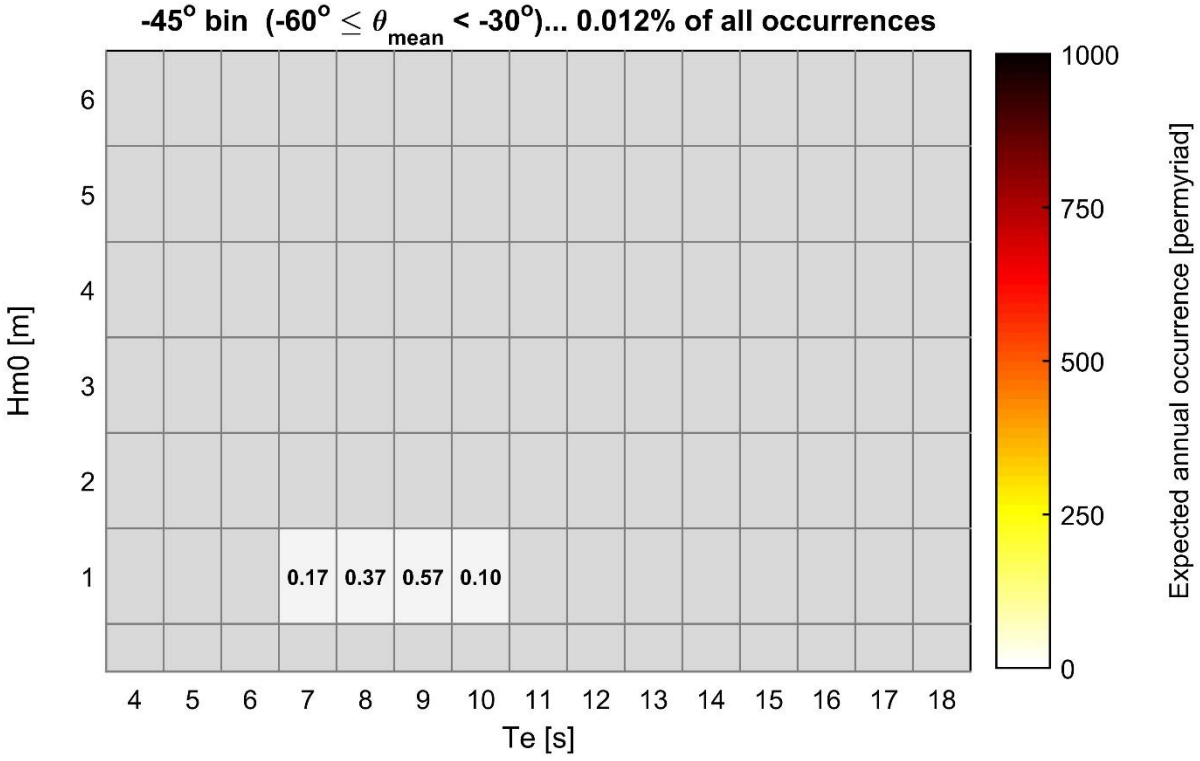

Figure 25 – Occurrence for -45° bin.

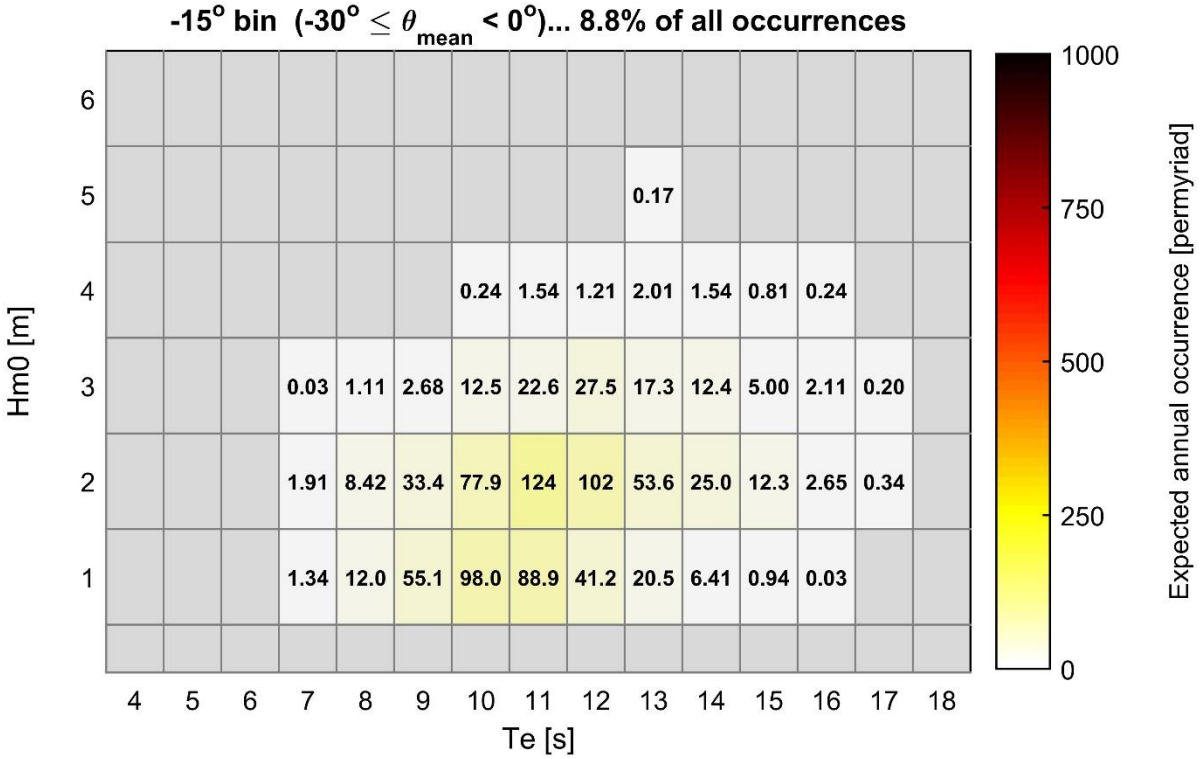

Figure 26 – Occurrence for -15° bin.

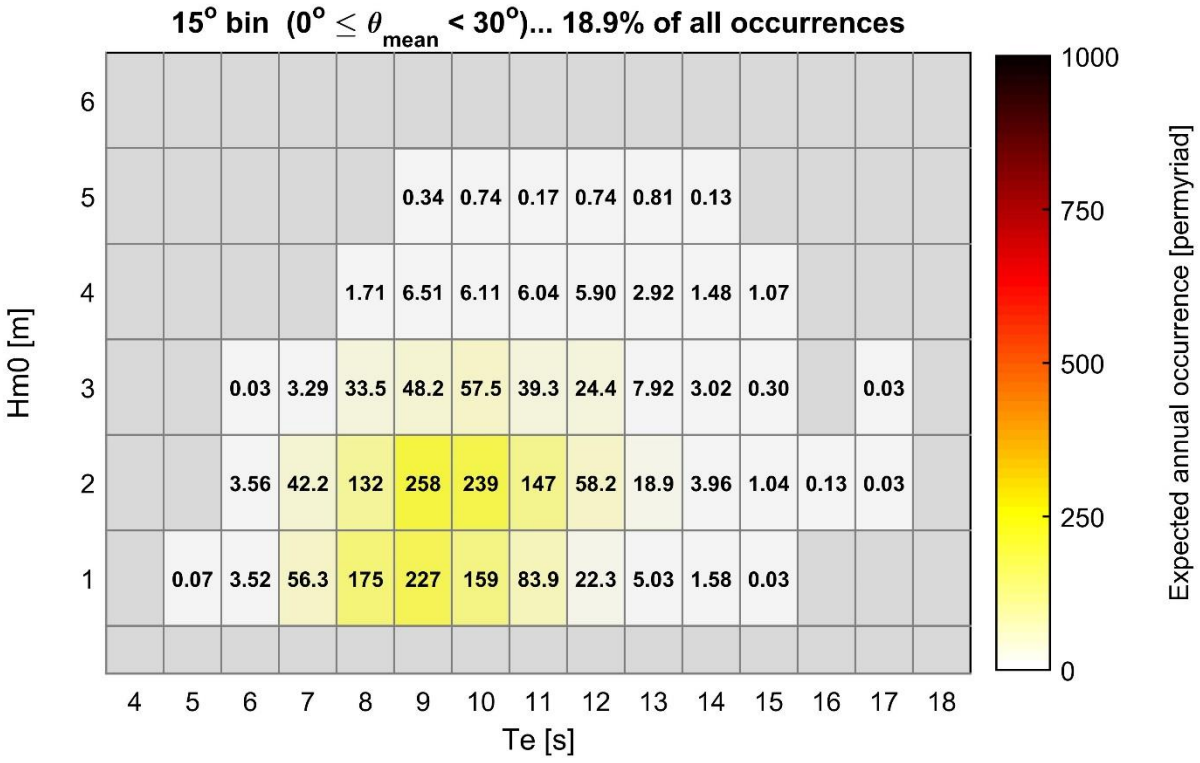

Figure 27 – Occurrence for 15° bin.

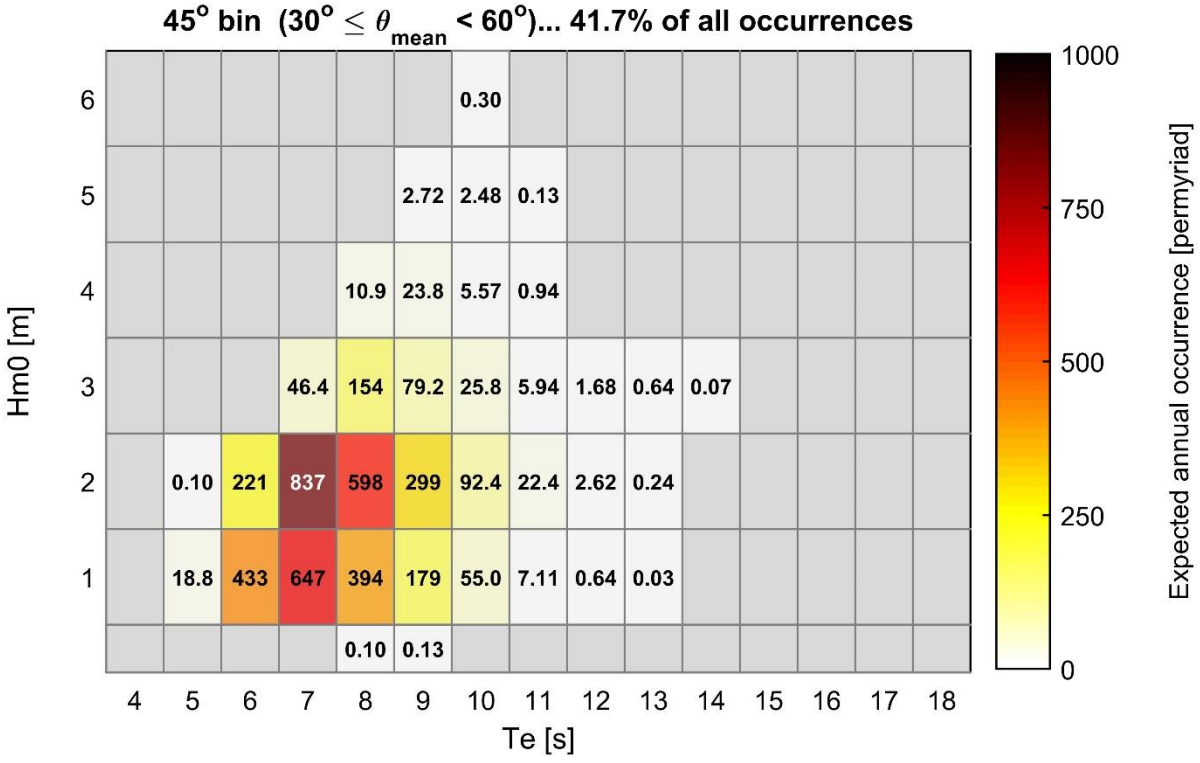

Figure 28 – Occurrence for 45° bin.

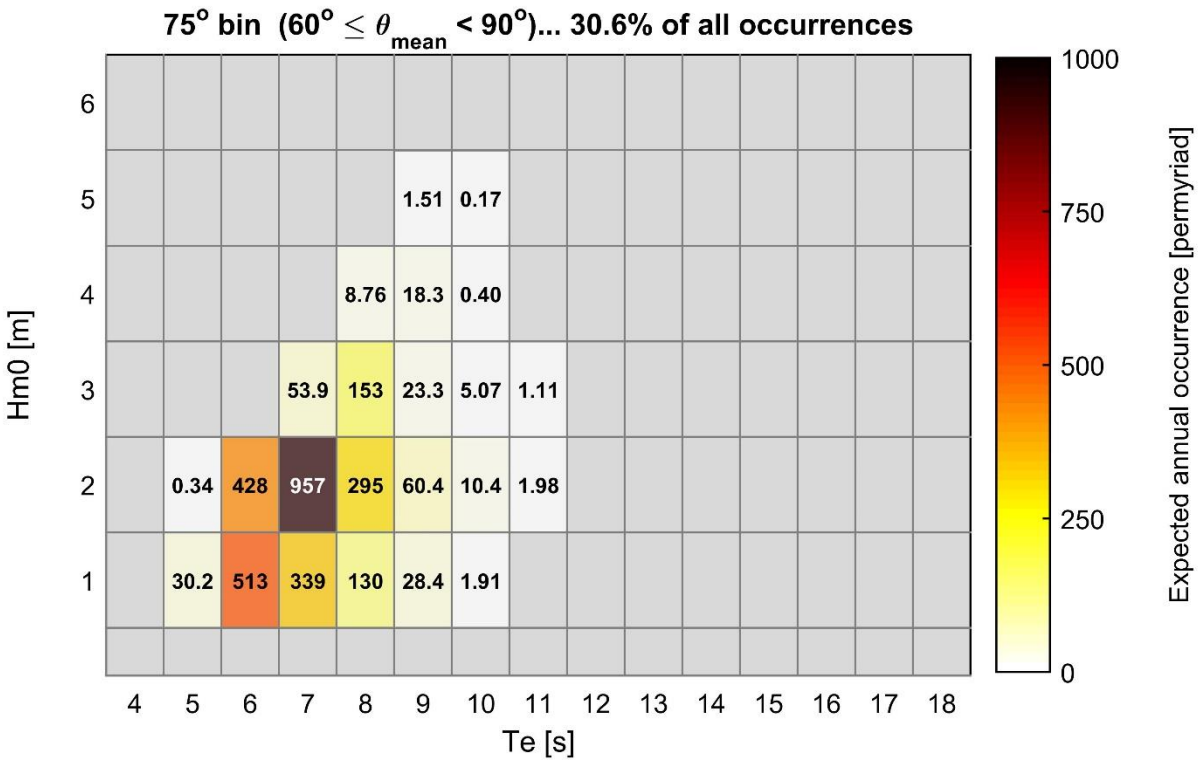

Figure 29 – Occurrence for 75° bin.

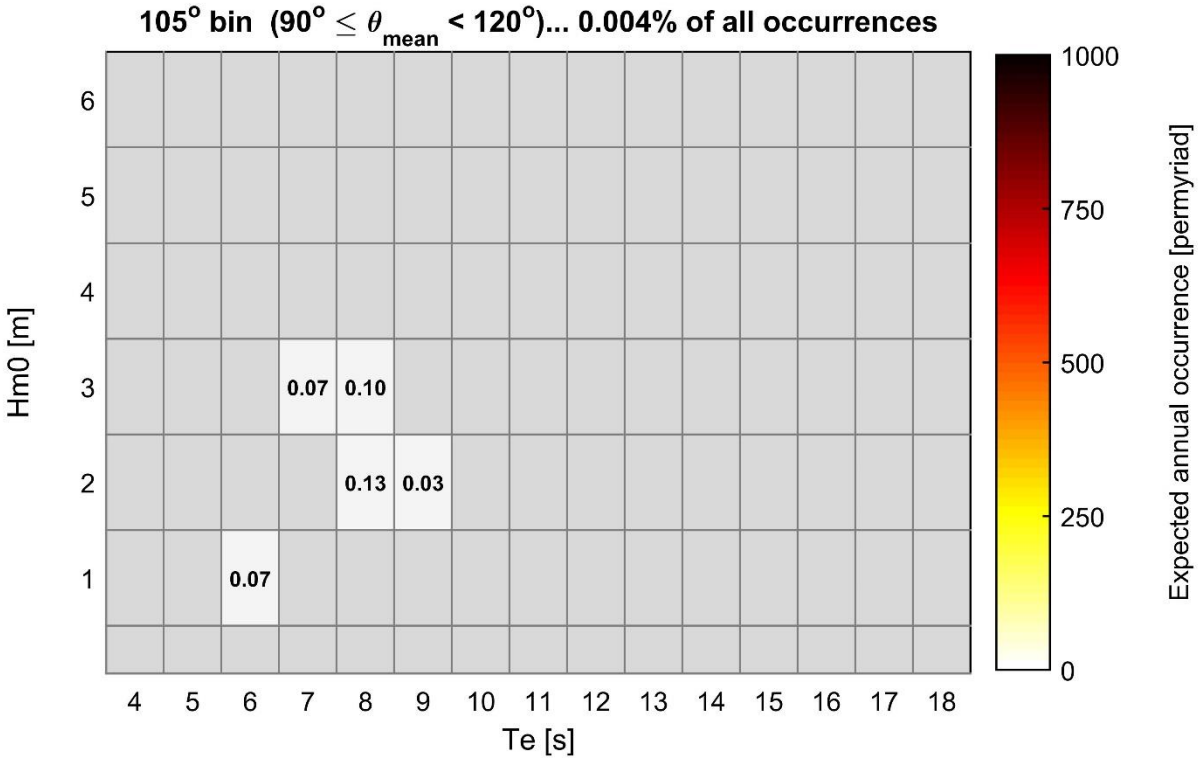

Figure 30 – Occurrence for 105° bin.

Table 7 – Mean sea state parameters for bins of non-zero occurrence.

Nominal			Mean			Occurrence	
Hm0 [m]	Te [s]	MDIR [°]	Hm0 [m]	Te [s]	MDIR [°]	[instances]	[permyriad]
0	8	45	0.49	8.3	47	3	0
0	9	45	0.49	8.6	41	4	0
1	5	15	0.89	5.4	29	2	0
1	5	45	1.12	5.4	55	561	19
1	5	75	1.13	5.4	66	900	30
1	6	-75	0.94	6.2	-82	5	0
1	6	15	1.15	6.2	23	105	4
1	6	45	1.25	6.1	53	12902	433
1	6	75	1.28	6.1	66	15296	513
1	6	105	1.06	6.4	94	2	0
1	7	-75	0.87	6.7	-64	3	0
1	7	-45	0.95	6.9	-52	5	0
1	7	-15	1.20	7.3	-7	40	1
1	7	15	1.21	7.2	22	1678	56
1	7	45	1.24	7.0	50	19299	648
1	7	75	1.26	6.9	66	10092	339
1	8	-45	0.82	8.2	-34	11	0
1	8	-15	1.09	8.2	-6	359	12
1	8	15	1.17	8.1	18	5228	175
1	8	45	1.21	8.0	46	11742	394
1	8	75	1.28	7.9	66	3875	130
1	9	-45	0.96	8.9	-33	17	1
1	9	-15	1.15	9.1	-7	1641	55
1	9	15	1.21	9.0	16	6765	227
1	9	45	1.24	8.9	43	5326	179
1	9	75	1.28	8.9	65	846	28
1	10	-45	1.18	9.8	-31	3	0
1	10	-15	1.20	10.0	-8	2920	98
1	10	15	1.24	10.0	14	4739	159
1	10	45	1.28	9.9	40	1638	55
1	10	75	1.36	9.7	63	57	2
1	11	-15	1.25	11.0	-9	2651	89
1	11	15	1.25	10.9	11	2501	84
1	11	45	1.30	10.8	36	212	7
1	12	-15	1.26	11.9	-10	1229	41
1	12	15	1.29	11.9	9	665	22
1	12	45	1.35	11.8	35	19	1
1	13	-15	1.29	12.9	-11	612	21
1	13	15	1.29	12.9	8	150	5
1	13	45	1.46	12.6	36	1	0
1	14	-15	1.27	13.9	-10	191	6
1	14	15	1.32	13.8	4	47	2
1	15	-15	1.33	14.8	-11	28	1
1	15	15	1.43	14.7	5	1	0
1	16	-15	1.50	15.7	-12	1	0
2	5	45	1.54	5.4	56	3	0
2	5	75	1.52	5.4	64	10	0
2	6	15	1.85	6.3	23	106	4
2	6	45	1.70	6.3	55	6576	221
2	6	75	1.70	6.2	65	12762	428
2	7	-15	1.83	7.2	-7	57	2

Nominal			Mean			Occurrence	
Hm0 [m]	Te [s]	MDIR [°]	Hm0 [m]	Te [s]	MDIR [°]	[instances]	[permyriad]
2	7	15	1.89	7.1	22	1258	42
2	7	45	1.85	7.0	52	24956	837
2	7	75	1.91	7.0	66	28528	957
2	8	-15	1.93	8.1	-7	251	8
2	8	15	1.88	8.1	19	3944	132
2	8	45	1.91	8.0	48	17829	598
2	8	75	1.96	7.9	66	8785	295
2	8	105	2.17	8.0	98	4	0
2	9	-15	1.84	9.1	-6	995	33
2	9	15	1.88	9.0	18	7690	258
2	9	45	1.89	8.9	43	8897	299
2	9	75	1.87	8.9	65	1801	60
2	9	105	2.19	8.6	91	1	0
2	10	-15	1.85	10.0	-7	2322	78
2	10	15	1.91	10.0	15	7138	239
2	10	45	1.90	9.9	41	2754	92
2	10	75	2.06	10.0	64	309	10
2	11	-15	1.87	11.0	-7	3700	124
2	11	15	1.90	10.9	12	4381	147
2	11	45	1.84	10.9	39	668	22
2	11	75	1.88	10.7	69	59	2
2	12	-15	1.93	12.0	-9	3052	102
2	12	15	1.96	11.9	10	1736	58
2	12	45	1.90	11.8	36	78	3
2	13	-15	1.97	12.9	-10	1599	54
2	13	15	1.98	12.9	7	562	19
2	13	45	2.35	12.9	33	7	0
2	14	-15	2.00	14.0	-10	745	25
2	14	15	2.00	13.9	4	118	4
2	15	-15	2.05	14.9	-10	366	12
2	15	15	1.93	14.8	4	31	1
2	16	-15	2.07	15.9	-11	79	3
2	16	15	1.98	15.9	4	4	0
2	17	-15	2.26	16.8	-5	10	0
2	17	15	2.46	16.8	3	1	0
3	6	15	2.55	6.4	17	1	0
3	7	-15	2.57	7.4	-4	1	0
3	7	15	2.71	7.3	22	98	3
3	7	45	2.70	7.3	51	1382	46
3	7	75	2.68	7.3	65	1607	54
3	7	105	2.71	7.4	94	2	0
3	8	-15	2.65	8.0	-6	33	1
3	8	15	2.85	8.1	22	999	34
3	8	45	2.86	8.0	49	4600	154
3	8	75	2.88	7.9	66	4567	153
3	8	105	2.65	7.6	101	3	0
3	9	-15	2.72	9.2	-7	80	3
3	9	15	2.86	9.0	20	1436	48
3	9	45	2.90	8.9	44	2362	79
3	9	75	2.93	8.8	65	694	23
3	10	-15	2.78	10.1	-6	374	13
3	10	15	2.86	10.0	16	1713	57
3	10	45	2.88	9.9	42	768	26
3	10	75	2.87	10.0	63	151	5

Nominal			Mean			Occurrence	
Hm0 [m]	Te [s]	MDIR [°]	Hm0 [m]	Te [s]	MDIR [°]	[instances]	[permyriad]
3	11	-15	2.84	11.0	-6	674	23
3	11	15	2.85	11.0	12	1170	39
3	11	45	2.79	10.9	38	177	6
3	11	75	3.21	10.6	62	33	1
3	12	-15	2.84	12.0	-8	819	27
3	12	15	2.88	12.0	9	728	24
3	12	45	3.00	12.0	35	50	2
3	13	-15	2.85	13.0	-9	515	17
3	13	15	2.91	12.9	6	236	8
3	13	45	2.85	12.6	35	19	1
3	14	-15	2.80	14.0	-10	371	12
3	14	15	2.99	14.0	8	90	3
3	14	45	2.57	13.6	31	2	0
3	15	-15	2.90	15.0	-11	149	5
3	15	15	3.23	14.6	21	9	0
3	16	-15	2.90	15.9	-10	63	2
3	17	-15	3.04	16.9	-3	6	0
3	17	15	2.67	17.0	1	1	0
4	8	15	3.69	8.2	20	51	2
4	8	45	3.72	8.3	52	325	11
4	8	75	3.72	8.2	63	261	9
4	9	15	3.74	9.0	23	194	7
4	9	45	3.90	8.9	50	709	24
4	9	75	3.87	8.9	65	544	18
4	10	-15	3.95	10.3	-2	7	0
4	10	15	3.81	9.9	20	182	6
4	10	45	3.94	9.9	46	166	6
4	10	75	3.88	9.8	64	12	0
4	11	-15	3.74	11.2	-4	46	2
4	11	15	3.86	11.0	17	180	6
4	11	45	4.13	10.8	42	28	1
4	12	-15	3.66	11.9	-6	36	1
4	12	15	3.92	12.0	11	176	6
4	13	-15	3.86	13.0	-5	60	2
4	13	15	4.02	13.0	5	87	3
4	14	-15	3.79	14.1	-8	46	2
4	14	15	4.05	14.1	7	44	1
4	15	-15	3.90	14.8	-10	24	1
4	15	15	4.10	14.8	7	32	1
4	16	-15	4.07	15.9	-5	7	0
5	9	15	4.63	9.1	17	10	0
5	9	45	4.73	9.1	53	81	3
5	9	75	4.70	9.3	65	45	2
5	10	15	4.69	10.2	18	22	1
5	10	45	4.98	9.8	52	74	2
5	10	75	4.74	9.5	65	5	0
5	11	15	4.79	10.5	23	5	0
5	11	45	4.58	11.0	39	4	0
5	12	15	4.61	12.1	14	22	1
5	13	-15	4.66	12.9	0	5	0
5	13	15	4.84	13.0	20	24	1
5	14	15	5.27	13.5	24	4	0
6	10	45	5.60	10.0	53	9	0

Calculation of Mean Spectra

Mean 2d spectra was calculated for each Hm0-Te-MDIR bin. To minimize "smearing", each spectrum was normalized prior to calculating the mean. The variance density of each spectra was normalized as

$$S_{fd,norm} = S_{fd}/(H_{m0}^2 T_e) \tag{4}$$

while the characteristic values of each frequency and directional spectral bin were normalized as

$$f_{norm} = f/f_e \quad \text{and} \quad \theta_{norm} = \theta - MDIR \tag{5}$$

where $f_e = 1/T_e$.

After calculating the mean of the normalized spectra for a given scatter table bin, the spectra and spectral scales were re-dimensionalized using the mean Hm0, Te and MDIR from the scatter table bin.

Data Structure

The data structure of the mean spectra and calculated parameters, as well as the individual spectra and calculated parameters, is given here.

The mean spectra and associated parameters are contained in meanSpec2d_mdir.mat:

- dir – characteristic values of spectral directions [deg]
- freq – characteristic values of spectral frequencies [Hz]
- meshDir – dir in meshgrid format [deg]
- meshFreq – freq in meshgrid format [Hz]
- seaStateIndices – 1xM cell array, each cell contains indices of individual spectra (see wetsSpec below)
- meanSpec1d – NxM array with N = number of mean spectra and M=length(freq) [m^2/Hz]
- meanSpec2d – NxMxQ array as above with Q=length(dir) [m^2/Hz/deg]
- meanParams – Nx13 table, columns listed below
    - Nspec – number of spectra in scatter matrix bin [ ]
    - nom_Hm0 – nominal Hm0 of bin [m]
    - nom_Te – nominal Te of bin [s]
    - nom_dirMean – nominal MDIR of bin [deg]
    - Hm0 – mean Hm0 of bin [m]
    - Te – mean Te of bin [s]
    - dirMean – mean MDIR of bin [deg]
    - calcd_Hm0 – Hm0 calculated from mean spectra [m]
    - calc_Te –Te calculated from mean spectra [s]
    - calcd_eps0 – spectral width calculated from mean spectra [ ]
    - calcd_J – wave power calculated from mean spectra [W/m]
    - calcd_dirMean – MDIR calculated from mean spectra [deg]
    - calcd_dirCoef – directionality coefficient calculated from mean spectra [ ]
- NOTE that the index in the first dimension of meanParams corresponds to the index of meanSpec1d, meanSpec2d and seaStateIndices

The individual spectra are contained in wetsSpec.mat:

- spectra1d – structure with the following fields

    - freq – characteristic values of spectral frequencies [Hz]
    - cg – group velocity associated with freq, at depth of 81m [m/s]
    - Sf – NxM array of variance density [m^2/Hz]
- spectra2d – structure with the following fields
    - freq – characteristic values of spectral frequencies [Hz]
    - dir – characteristic values of spectral directions [deg]
    - meshDir – dir in meshgrid format [deg]
    - meshFreq – freq in meshgrid format [Hz]
    - Sfd – NxMxQ array of variance density [m^2/Hz/deg]

Calculated parameters are contained in wetsParams_mdir.mat:

- depth – depth used in calculations [m]
- params – Nx13 table
    - utcTime – time of modeled sea state data record [UTC time]
    - Hm0 – significant wave height [m]
    - Te – energy period [s]
    - Tz – mean zero crossing period [s]
    - T01 – mean period [s]
    - Tp – peak period [s]
    - eps0 – spectral width [ ]
    - J – wave power [W/m]
    - dirJmax – direction of maximum directionally resolved wave power [deg]
    - dirMean – mean direction [deg]
    - dirPeak – peak direction [deg]
    - dirCoef – directionality coefficient
    - Ss – significant steepness [ ]